IDŐJÁRÁS

QUARTERLY JOURNAL
OF THE HUNGARIAN METEOROLOGICAL SERVICE

CONTENTS

****

http://www.met.hu/firat/ido-e.html

VOL. 104 * NO. 4 * OCTOBER–DECEMBER 2000

IDŐJÁRÁS

Quarterly Journal of the Hungarian Meteorological Service

Editorial Office: P.O. Box 39, H-1675 Budapest, Hungary or
Gilice tér 39, H-1181 Budapest, Hungary
E-mail: prager@met.hu or *antal@met.hu*
Fax: (36-1) 290-7387

Subscription by

mail: IDŐJÁRÁS, P.O. Box 39, H-1675 Budapest, Hungary;
E-mail: prager@met.hu or *antal@met.hu*; *Fax: (36-1) 290-7387*

IDŐJÁRÁS

Quarterly Journal of the Hungarian Meteorological Service
Vol. 104, No.4, October–December 2000, pp. 219–239

The application of ALADIN model for storm warning purposes at Lake Balaton

Imre Bartha[1], **András Horányi**[2] and **István Ihász**[2]

[1]*Hungarian Meteorological Service, Storm Warning Observatory, Vitorlás u. 17, H-8600 Siófok, Hungary; E-mail: bartha.i@met.hu*

[2]*Hungarian Meteorological Service, P.O. Box 38, H-1525 Budapest, Hungary; E-mail: horanyi.a@met.hu; ihasz.i@met.hu*

(Manuscript submitted for publication 20 January 2000; in final form 8 May 2000)

Abstract—Strong and stormy winds are the most dangerous weather phenomena in the resort region of Lake Balaton, and that is why the weather warnings are of great importance for the protection of life and property. In summer the wind storms breaking out suddenly in the area of Lake Balaton are generally associated with thunderstorms.

In wind forecasting, one of the most difficult tasks is to predict the degree of wind strengthening associated with thunderstorms, as it may vary according to the synoptic situation. This paper studies how correct and useful information is available in the products of the limited area numerical weather prediction model ALADIN for forecasting the spatial and temporal intensity of organised convection using an interactive nowcasting decision-making procedure. The procedure provides a more objective foundation for storm warnings at Lake Balaton. The obtained results are completed by the statistical investigation for the application of meteograms to the storm warning practice.

Key-words: very short range forecast, nowcasting, storm warning, decision-making procedure, limited area numerical weather prediction model, parameterization of organised convection, meteogram.

1. Introduction

Strong and stormy winds are the most dangerous weather phenomena in the resort region of Lake Balaton. In summer the wind storms breaking out suddenly in the area of the lake are generally associated with thunderstorms, that is why the weather warnings are of great importance for the protection of life and property. The Storm Warning Observatory (SWO) at Lake Balaton of the Hungarian Meteorological Service (HMS) was founded with the aim of

providing such warnings. In the high season the holidaymakers, sailors and surf-riders require

(1) information on the present weather situation,
(2) a very short range forecast valid for max. 12 hours and
(3) warnings with the help of the National Directorate General for Disaster Management of Ministry of the Interior 1–2 hours ahead of expected wind gusts [V(max)] exceeding 12 or 17 m s^{-1}.

In order to solve the 2nd and the 3rd tasks complying with the requirements, we need a correct very short range forecasting model. On the basis of our experiences, the limited area model (LAM) ALADIN is a good candidate for the precise forecasting of the intensity and period of instability connected to convective activity.

2. Application of ALADIN products at SWO of HMS

The HMS has been taking part in the ALADIN international collaboration initiated by Météo France since 1991. The result of this collaboration is the limited area spectral hydrostatic numerical weather prediction model ARPEGE/ALADIN (*Horányi et al.,* 1996), which is used operationally at the Hungarian Meteorological Service. The ALADIN/LACE version of the model is operationally exploited in Prague (for a domain over continental Europe) providing not only forecasting products but also initial and lateral boundary conditions for the workstation version of ALADIN (called ALADIN/HU, which covers a domain over the Carpathian Basin). At the time of the experiments the resolution of the ALADIN/LACE and ALADIN/HU models were 14.7 km and 11 km, respectively. The products of the ALADIN/LACE regional and ALADIN/HU local models are available for the forecasters through the HAWK (Hungarian Advanced WorKstation) visualization system developed by US–Hungarian co-operation (*Horváth et al.,* 1998).

The storm forecast obviously utilizes shorter range forecast (valid for max. 12 hours) due to its nowcasting character. In this field, the possible further application of ALADIN products opened a new perspective with respect to the dangerous quickly evolving small scale weather systems (*Banciu* and *Geleyn,* 1998).

In wind forecasting, one of the most difficult tasks is to predict the degree of wind strengthening associated with thunderstorm, as it may vary according to the synoptic situation. It is known by storm forecasting experience that the summer wind storms breaking out suddenly in the region of Lake Balaton are generally associated with thunderstorms. That is why during the 1980s (*Bartha,* 1987) and later in the 1990s (*Bartha et al.,* 1998) an interactive

decision-making procedure *(Fig. 1)* was developed in order to estimate which wind category the maximum wind gusts [V(max) in units of m s^{-1}] belong to. The categories are the following: no warning [D(0): V(max) < 12 m s^{-1}], alert [D(1) a: 12 m $s^{-1} \leq$ V(max) ≤ 17 m s^{-1}] and storm warning [D(2): V(max) $>$ 17 m s^{-1}].

In Fig. 1 it can be seen that the very short range forecast for the region of Lake Balaton serves as a basis for decision-making on storm warning. The method combines the conventional data with the approach of using radar information. During the decision-making procedure as a monitoring, we use a simple parameter, the so-called cooling rate (ΔT). This monitoring procedure is based on the idea that there is a close relationship between the temperature decrease (ΔT) induced by downdraft and the maximum wind velocity at the surface in non-frontal thunderstorms (*Fawbush* and *Miller,* 1954). We have used the recent improvements of the convection parameterization scheme of ARPEGE/ALADIN in order to investigate the capability of the model for describing the spatial and temporal intensity of convective activity. This evaluation helps to decide how the results of the ALADIN model can be used as input data for the nowcasting decision-making procedure (*Bartha,* 1998).

3. Experiments and data sets

3.1. Experiments

The most important parts of our present investigations are

(1) to asses the impact of the most recent modifications of the convection parameterization scheme for ALADIN based on *Bougeault* (1985), i.e.,

- introduction of downdraft parameterization, based on *Ducrocq* and *Bougeault* (1995) — see *Banciu* and *Geleyn* (1998),
- momentum parameterization, based on *Kershaw* and *Gregory* (1997) as well as *Gregory et al.* (1997) implemented by *Gerard* (1998),
- limitation of humidity convergence by subtracting stratiform precipitation for the available humidity of convection scheme,
- tuning of some free parameters of the convection scheme,

in order to obtain a realistic description for the intensity of organised convection in space and time;

(2) to study how correct information is available in ALADIN/HU meteograms for two local points of Lake Balaton in comparison to the real data during the selected unstable weather conditions.

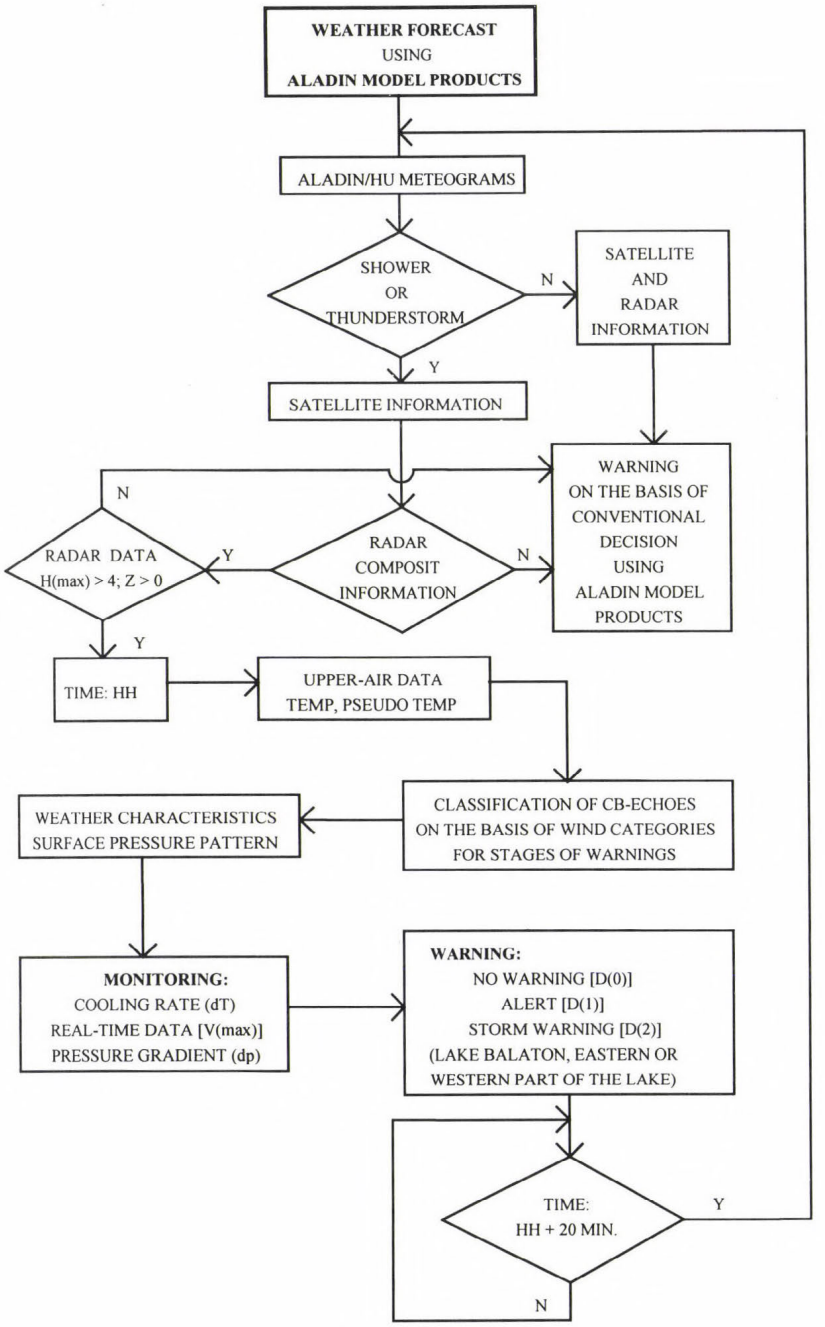

Fig. 1. Nowcasting decision-making procedure using ALADIN products for forecasting the maximum wind gusts associated with thunderstorms.

3.2. Data sets

In order to solve the above mentioned tasks, some active cold fronts associated with thunderstorms (6 cases) and convective systems [local thunderstorm situations (2 cases), convergence zones (5 cases), squall lines (2 cases)] were studied over the western part of Hungary (*Table 1*). These wind–hazardous weather situations were collected in 1998 during the period from May to August.

Table 1. Thunderstorm-hazardous weather situations in the western part of Hungary collected in 1998 during the period from May to August (the squall line cases studied are in bold face)

Date	Period (UTC)	Phenomenon
May 13	12 – 15	convergence zone
May 21	12 – 18	convergence zone
May 29	12 – 18	local thunderstorms
June 01	09 – 15	weak cold front associated with thunderstorms
June 03	15 – 21	convergence zone
June 08	12 – 21	cold front associated with thunderstorms
June 22	**09 – 18**	**squall line and cold front**
June 28	12 – 21	cold front associated with thunderstorms
June 30	15 – 21	convergence zone
July 27-28	**21 – 03**	**squall line and cold front**
July 28	06 – 15	cold front associated with thunderstorms
July 31–August 01	21 – 01	convergence zone
August 05	00 – 09	cold front associated with thunderstorms
August 19	06 – 12	local thunderstorms
August 19	15 – 21	cold front associated with thunderstorms

The following data were used for the investigations:

- hourly (in some cases every quarter of an hour) composite radar pictures from the detection region of Hungary, where the radar is of MRL–5 type and worked on the wavelength of 10 or 3 cm producing information for square elements of 2×2 km^2;
- observed data for Cu- or Cb-clouds (SYNOP code: $C_L = 2$, 3 or 9) and some significant convective weather phenomena (shower, thunderstorm, hailstorm, wind gust connected with Cb-clouds of 7 m s^{-1} or stronger) of 3 principal synoptic stations and 8 automatic meteorological stations transmitting real-time wind information around Lake Balaton;
- three hourly surface meso-synoptic and twelve hourly high level (850, 700 and 500 hPa) operational charts analysing the development and movement of frontal and convective systems over the region of West Hungary;

- vertical profiles in traditional emagram form for the two selected squall line cases;
- ALADIN/LACE pseudo–TEMP messages visualised in time cross-sections for two stations (Siófok and Keszthely) of local interest;
- ALADIN/HU meteograms for two stations (Siófok, Keszthely) of local interest;
- output results (e.g., forecasting charts on various pressure levels with hourly frequency, like vertical velocity at 700 hPa level, 10m wind velocity, 2m temperature, the amount of precipitation, etc.) of the experimental version of the ALADIN model.

4. Results and discussion

We used the above described modifications of the convection scheme (see paragraph 3.1) trying to tune the free parameters of the scheme in order to obtain a better agreement with the observed evolution (in space and time) of the squall lines. For the experimental version of ALADIN/HU, we adopted a bit finer resolution than the operational resolution ($\Delta x = 11$ km) of ALADIN/HU model having 10 km horizontal resolution with 27 vertical levels. The domain (*Fig. 2*) remained, as it is for the operational version and some results were visualized for a zoomed area over Hungary. The forecast base was 00 UTC in the first case and it was 12 UTC in the second case. The maximum forecasting time was +18 hours and the post-processing step was 1 hour.

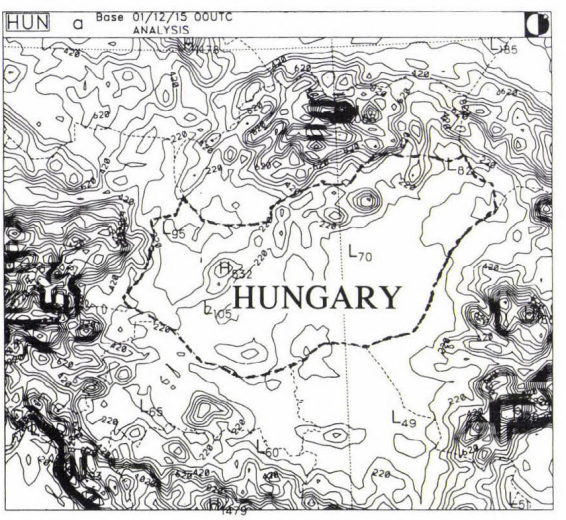

Fig. 2. ALADIN/HU operational domain over the Carpathian Basin with the model orography (unit in meter).

4.1.1 The first case—synoptic situation and associated weather feature

For the purpose of this experiment a rather strong squall line case was selected which developed ahead of a cold front on June 22, 1998. We intentionally chose this interesting case as a first one because it developed very suddenly within one hour and it was limited to a small territory. Sharp squall lines can be forecasted by the other models (e.g., DWD or ECMWF models), too.

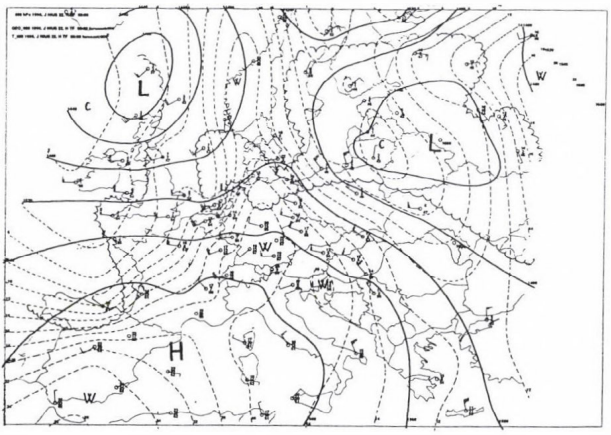

Fig. 3a. HMS analyses of geopotential (solid lines in gpdam) and temperature (dashed lines in °C) at 850 hPa for 00 UTC June 22, 1998 (Legends: L=low, H=high, w=warm, c=cold).

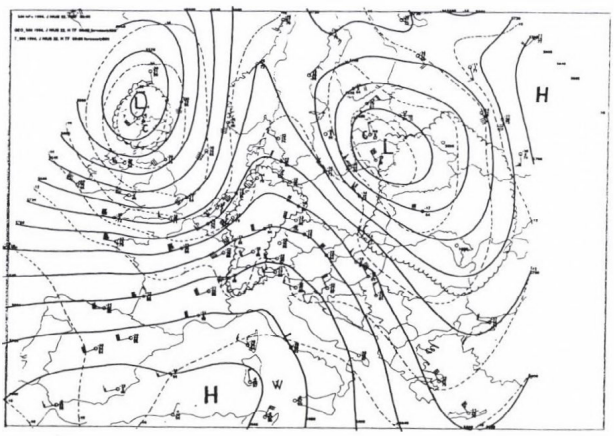

Fig. 3b. HMS analyses of geopotential (solid lines in gpdam) and temperature (dashed lines in °C) at 500 hPa for 00 UTC June 22, 1998 (Legends: L=low, H=high, w=warm, c=cold).

According to the large scale synoptic situation, a cold front reached the line of Hamburg–Frankfurt–Marseille by 00 UTC and ahead of it on the higher levels (*Fig. 3a,b*) very warm, relatively humid and unstable air

accumulated over Central and Southern Europe. A radiosonde ascent from Vienna also verified this fact at 00 UTC. Later, on the basis of surface meso-analyses (*Fig. 4a)*, this cold front stopped in Austria near the western border of Hungary. At 12 UTC, a squall line erupting very intensive thunderstorms could be analysed (Fig. 4a). In this situation identifying the first weak radar echoes at 10:30 UTC, the storm warning service ordered warnings [in Fig. 1: D(2)] around Lake Balaton. One hour later severe thunderstorms occurred with hailstones in the western part of the lake and the maximum wind gusts exceeded 22 m s^{-1}. In the mean time, the squall line moved southward at a speed of about 35 km h^{-1} and therefore became more dangerous. According to the radar measurements, the maximum reflectivity factor changed from 20–30 dBZ to maximum 62,5 dBZ and the top of radar echoes reached 11–13 km within half an hour (*Fig. 4b*). Later the cold front system accelerated and merged into the squall line at about 15 UTC.

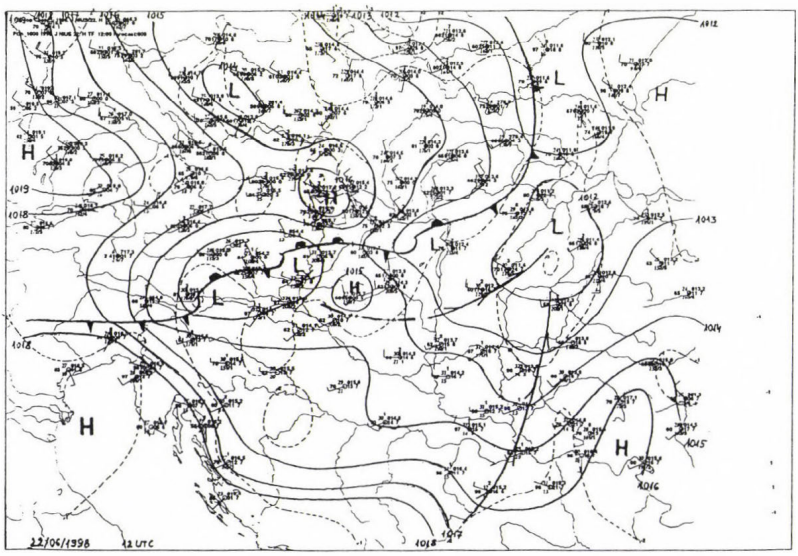

Fig. 4a. HMS meso-analyses for the msl-pressure (hPa) at 12 UTC on June 22, 1998 (Legends: H = High, L = Low)

The squall line caused huge damages in buildings, trees, etc., on the lake-shore and on the lake. Far from the lake, to S-SW of it, about 4–5 villages were flooded with muddy water causing damages in the buildings, gardens and

the roads. In these areas, the maximum amount of precipitation was 82 mm, whilst the average monthly amount is 75 mm.

On the basis of the above-mentioned traditional synoptic data sources at 00 UTC, we managed to forecast the maximum air temperature, the thunderstorms, the wind strengthening and the change of wind direction by afternoon in the region of Lake Balaton, but naturally we could not forecast the exact time and place of thunderstorm eruptions.

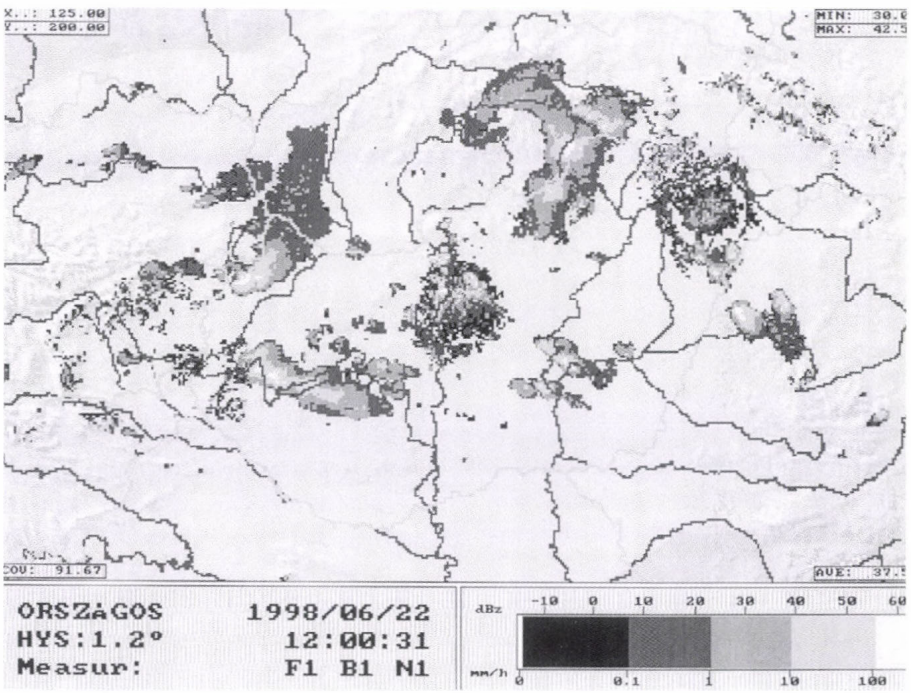

Fig. 4b. HMS composite weather radar image (reflectivity in dBZ) at 12 UTC on June 22, 1998 over the Carpathian Basin.

4.1.2 The first case—impact of the modification of parameterization for convection

This section reports on the results of the simulation for the first selected squall line case. Six experiments (identified as SH10, SH11, SH12, SH13, SH14 and SH15) were carried out to test the ALADIN model's sensitivity regarding the parameterization among the six ones. Only the best version is shown. The

results were compared to the observations considering the intensity and position of the squall line.

Parameters used for experiments as it appeared in the ALADIN model:

❶ The threshold level (in Pa), above it the horizontal diffusion was enhanced.
❷ Logical switch to activate the subtraction of large scale precipitation from the humidity convergence available for the convection scheme.
❸ Logical parameter to switch on the parameterization of downdraft.
❹ Logical parameter for evaporation convection under the cloud basis.
❺ Coefficient of pressure gradient for *Kershaw* and *Gregory* parameterization—the reasonable thresholds for this coefficient were still not finally defined at the time of the experiments.
❻ Entrainment rate at the cloud basis.
❼ Downdraft parameter—the fraction of precipitation evaporated to produce the downdraft.

The best experiment with parameter tuning:

Experiment	❶	❷	❸	❹	❺	❻	❼
SH15	0.0	NO	NO	YES	< 1	0.4E–4	0.25

Experiment SH15 (which is basically the operational version, except the value of the first parameter) without downdraft, was proved to be the best. The development of the convergence zone and later gust front is simulated well enough by 10m wind (m s^{-1}) distribution (*Fig. 5a*) in comparison to the real radar measurements (Fig. 4b) and surface meso analyses (Fig. 4a). In Fig. 5a it can be seen that the wind changed from SW to NW behind the line and increased in a small degree. The gust front separates from the cold front system and progresses parallel with the cold front. The distribution of vertical velocity (Pa s^{-1}) also shows the two systems but the core of upward motions are stronger along the cold front than along the convergence line (*Fig. 5b*).

The cooling (not shown) behind the squall line is also simulated but there was an unrealistically big difference between the 2m air temperature and the surface water temperature of Lake Balaton. At that time (at 12 UTC on the June 22) the real water temperature was 23°C (at 1 m depth below the water surface) vs. the simulated surface water temperature value of 17°C.

On the basis of the six experiments it seems that the model is not very sensitive to the tuning of the free parameters of the scheme in this selected squall line case. It was also noticed that the modifications of the convection scheme led to a noisy vertical velocity field in the northern part of the ALADIN/HU operational domain.

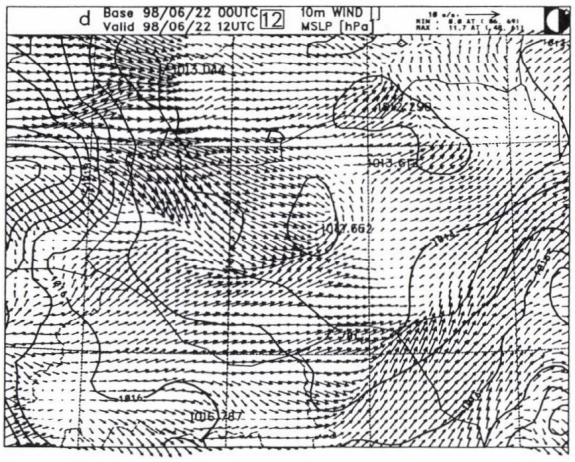

(a)

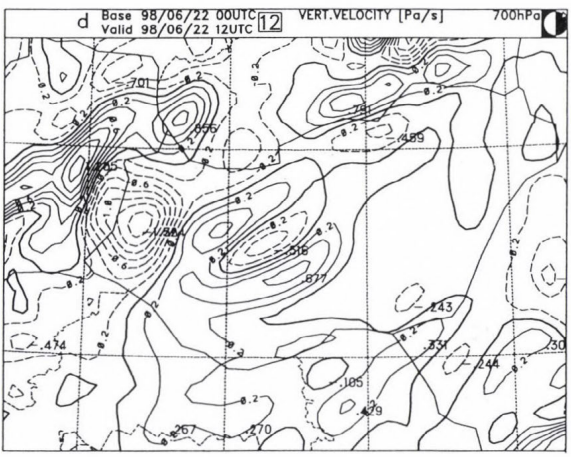

(b)

Fig. 5. Distribution in space and time (at 12 UTC) for 10m wind (m s^{-1}) together with the msl-pressure field (*a*) and for vertical velocity (Pa s^{-1}) at 700 hPa (*b*), simulated by ALADIN model experiments SH15 for June 22, 1998.

4.2.1 The second case – synoptic situation and associated weather feature

A shallow cyclone weather situation took place over West Europe between 0 and 10 degrees of longitude at 00 UTC on the operational surface chart (not shown) in the line of Edinburgh–London–Nantes–La Coruna. 12 hours later a fairly warm, relatively humid and unstable air-mass reached the western part of the Alps on the higher levels (*Fig. 6a,b*) ahead of the cold front. A radiosonde ascent from Zagreb also verified this unstable stratification near

Hungary at 12 UTC. In the mean time, the cold front moved towards east and reached the line of Wroclaw–Vienna–Klagenfurt at 21 UTC. Later the cold front reached the eastern part of the Alps where it stopped, and a warm wave occurred along the northern part of the frontal zone *(Fig. 7a)*. Ahead of this zone, a quick squall line began to evolve near the western border of Hungary along the line of Szentgotthárd–Nagykanizsa and moved from SW to NE direction nearly parallel with the stopping cold front. The amount of precipitation was between 1 and 7 mm in the region of Lake Balaton. Large amount of precipitation was measured along the frontal zone in the northern part of Hungary. The maximum wind gust associated with thunderstorms was only 15 m s^{-1} around Lake Balaton. The cold front zone merging in the squall line left the western part of Hungary after 03 UTC.

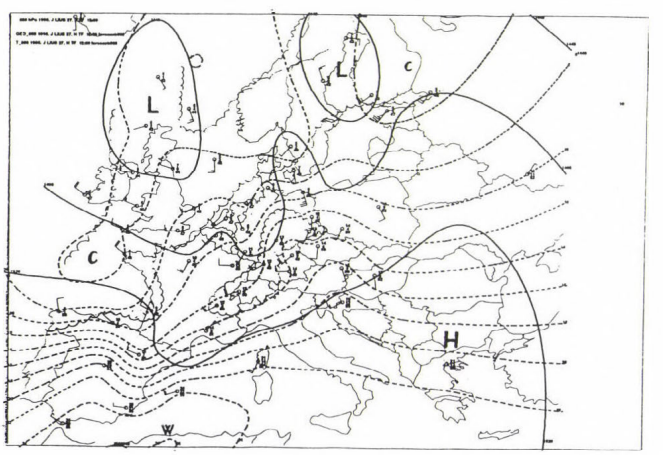

Fig. 6a. HMS analyses of geopotential (solid lines in gpdam) and temperature (dashed lines in °C) at 850 hPa for 12 UTC on July 27, 1998 (Legends: L=low, H=high, w=warm, c=cold).

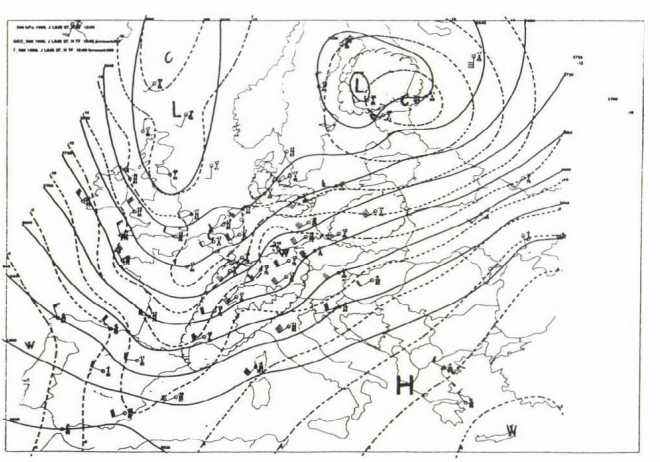

Fig. 6b. HMS analyses of geopotential (solid lines in gpdam) and temperature (dashed lines in °C) at 500 hPa for 12 UTC on July 27, 1998 (Legends: L=low, H=high, w=warm, c=cold).

On the basis of the synoptic data sources at 12 UTC, we managed to forecast the thunderstorms by night and the change of wind direction by the second part of the night in the region of Lake Balaton. Of course, we were not able to forecast the exact time and place of thunderstorm eruptions from these data sources. The ALADIN/HU meteograms for two local points (Siófok, Keszthely) of Lake Balaton were able to forecast the period of maximum intensity of lability very well. For the first time, the developing squall line was detected to SW of the lake by radar at 23:15 UTC. 15 minutes later *(Fig. 7b)*, the squall line reached the western part of Lake Balaton. This sharp and narrow instability line left the eastern part of the lake at 00:45 UTC. The length of the line varied between 150 and 200 km, its width varied between 20 and 40 km.

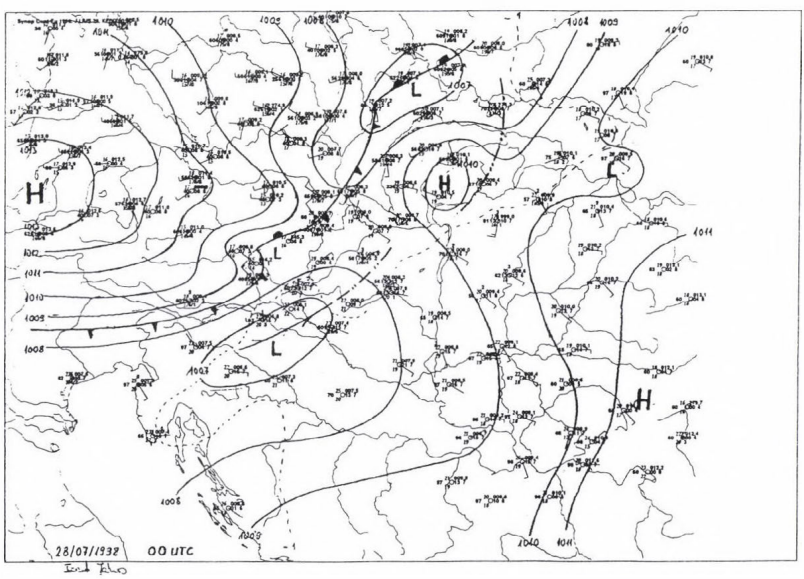

Fig. 7a. HMS meso-analyses at 00 UTC on July 28, 1998 (Legends: H=high, L=low).

4.2.2 The second case—the results by physical coefficient tuning in comparison to real data

The physical parameters used for the experiments were the same as in 4.1.2. Seven experiments (identified as TH00, TH01, TH02, TH03, TH04, TH05

and TH06) were carried out to test the ALADIN model's sensitivity regarding the parameterization among the seven ones. Only the best version is shown.

The best experiment with parameter tuning:

Experiment	❶	❷	❸	❹	❺	❻	❼
TH03	50000	YES	YES	NO	< 1	0.6E-4	0.25

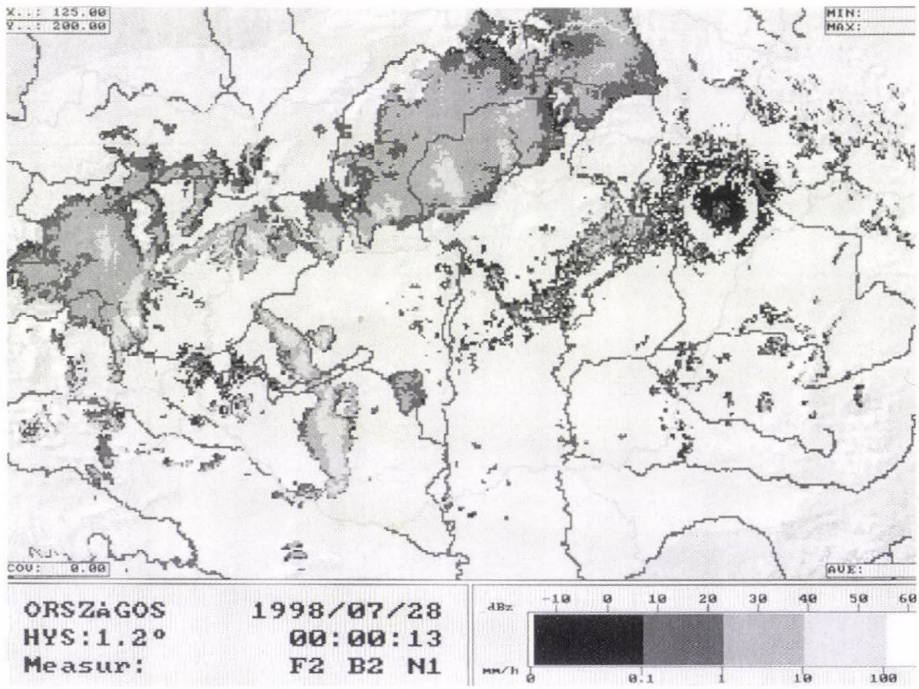

Fig. 7b. HMS composite weather radar image (reflectivity in dBZ) at 00 UTC on July 28, 1998 over the Carpathian Basin.

Experiment TH03 proved to be the best one with downdraft parameterization. The development of the gust front was simulated well enough by the 10m wind distribution with the mean sea level pressure structure (*Fig. 8a*). The results were compared to the suitable surface meso-analyses (Fig. 7a) and radar image (Fig. 7b). It can be seen that the position of the squall line at 00 UTC is nearly the same. Fig. 8a demonstrates very well that the wind direction changed from SW to NW behind the line and increased in larger degree. The gust front separates from the cold front system well enough and

progresses parallel with the cold front. The pattern of vertical velocity also shows the two systems (*Fig. 8b*), but the cores of upward motions are stronger along the cold front than the squall line.

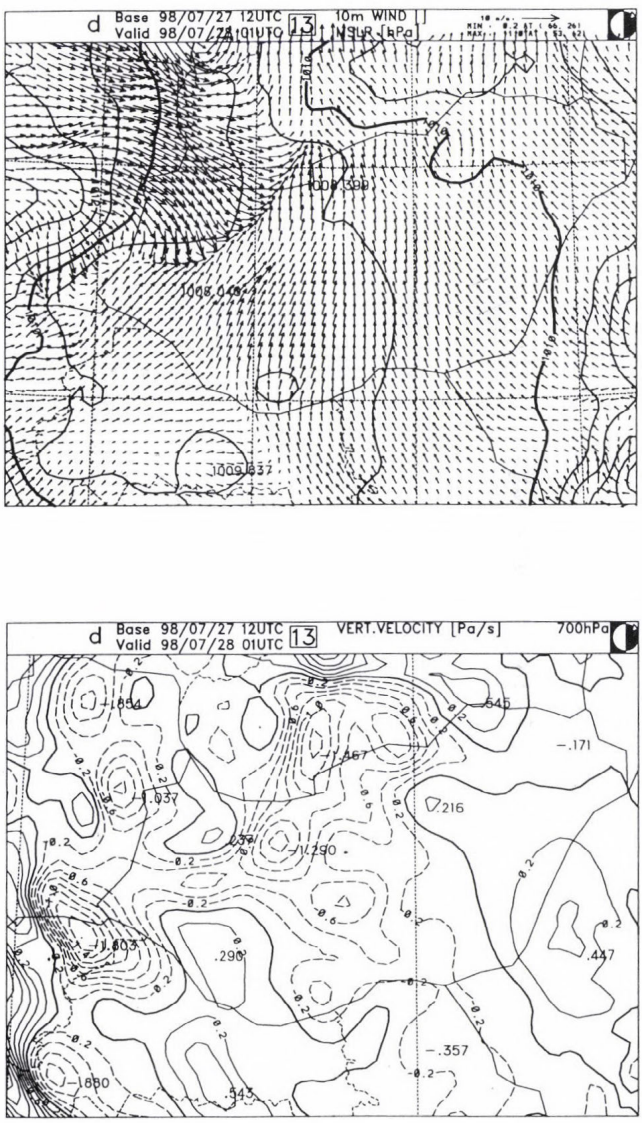

Fig. 8. Distribution in space and time (at 01 UTC) for 10m wind (m s^{-1}) together with the msl-pressure field (*a*) and for vertical velocity (Pa s^{-1}) at 700 hPa (*b*) simulated by ALADIN model experiments TH03 for July 28, 1998.

4.3 Studying how correct information is available according to ALADIN/HU meteograms for two local points of Lake Balaton in comparison to real data

We compared in space (Siófok, Keszthely) and time (every 3 hours) the forecasts according to ALADIN/HU meteograms of total cloud cover [N(F)], convective cloud cover [NL(F)], 10m wind velocity [V(F)], 2m temperature [T(F)] to the real synoptic observations [N(O), NL(O), V(O), T(O), respectively] for the thunderstorm-hazardous weather situations (Table 1) — see *Fig. 9.*

4.3.1 Forecast of total cloud cover [N(F)]

On the basis of this investigation, it was clear that there was no statistical difference between the forecasts of total cloud cover [N(F)] for two local points (Siófok and Keszthely) in the region of Lake Balaton. The mean error [ME/N(F)/] for the forecast of total cloud cover was one octant as an underestimation with standard deviation of two octants (*Fig. 9a).*

4.3.2 Forecast of convective cloud cover [NL(F)]

Statistically we did not find any difference between the results as for the two local points (Siófok, Keszthely) in the region of Lake Balaton. The mean error [ME/NL(F)/] for the forecast of convective cloud cover was near to zero with relatively big standard deviation (3 octants, *Fig. 9b*). This fact is remarkable for forecasting the convective periods.

4.3.3 Forecast of 10m wind velocity [V(F)]

On the basis of this statistical evaluation investigation, there were significant differences in wind forecasts belonging to the two local points (Siófok, Keszthely). The 10m wind velocity forecasts for Siófok [VS(F)] were underestimated by ALADIN/HU meteograms (*Fig. 9c*). The mean error [ME/VS(F)/] was -1.25 m s^{-1} with standard deviation of 3.10 m s^{-1}. One of the possible explanations for the underestimation of wind velocity may be that the grid point (in ALADIN model) is not in suitable agreement with the real climatic characteristics of Siófok. The fact is that the meteorological station in Siófok stands close to the lake (10 meters from the lake) and that is why the influence of the water surface is significant particularly during no (pressure) gradient weather situations. This influence depends on the direction of air circulation between lake and land. Namely, in day-time the wind usually blows from the lake and in this way, if thunderstorms are able to break out north of Siófok, the wind gusts induced by cold air spreading out at the surface under a thundercloud could become stronger and stronger over the relatively smooth

water surface. At the same time the forecasts [VK(F)] for Keszthely were overestimated. The mean forecast error [ME/VK(F)/] was +0.59 m s^{-1} with standard deviation of 1.78 m s^{-1} (*Fig. 9d*).

The forecast in space (Siófok, Keszthely) and time (every 3 hours) for the change of wind direction and the course of wind strengthening are equivalent of the real observations in quality. Unfortunately the degree of wind strengthening is significantly underestimated in Siófok, and at the same time it is overestimated in Keszthely.

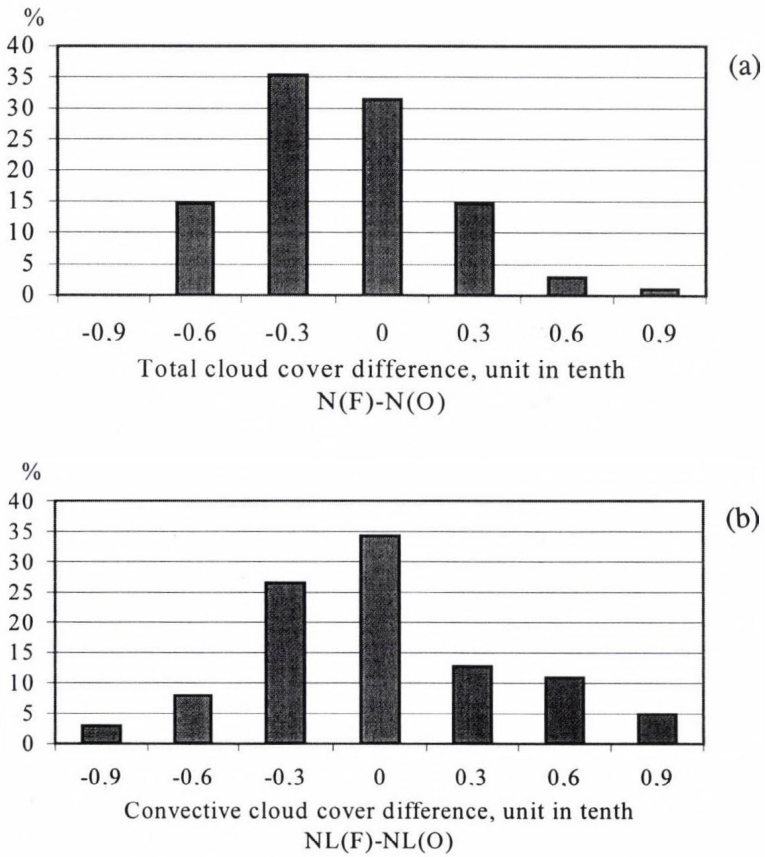

Fig. 9. Differences between the forecasts given by ALADIN/HU meteograms and observations (for all the cases in Table 1) as a function of percentage of cases for (*a*) total cloud cover (N(F), unit in tenth), (*b*) convective cloud cover (NL(F), unit in tenth), (*c*) 10m wind velocity in Siófok (VS(F), unit in m s^{-1}), (*d*) 10m wind velocity in Keszthely (VK(F), unit in m s^{-1}) and (*e*) 2m temperature (T(F), unit in °C). (*f*) Mean error [ME/T(F)] for the forecast by ALADIN/HU meteograms) of 2m temperature (°C) with respect to observations as a function of forecast range.→ →

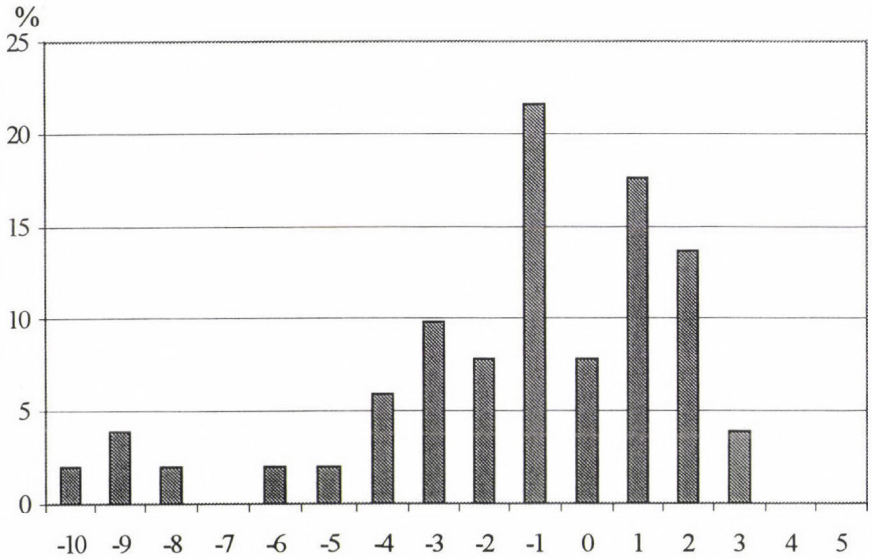

(c)

10m wind velocity difference (m s^{-1}) in Siófok
VS(F)–VS(O)

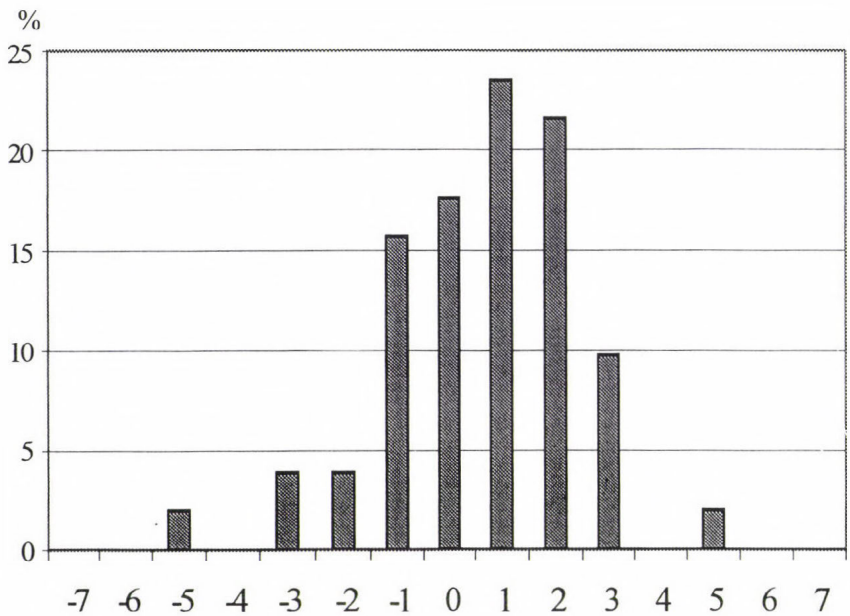

(d)

10m wind velocity difference (m s^{-1}) in Keszthely
VK(F)–VK(O)

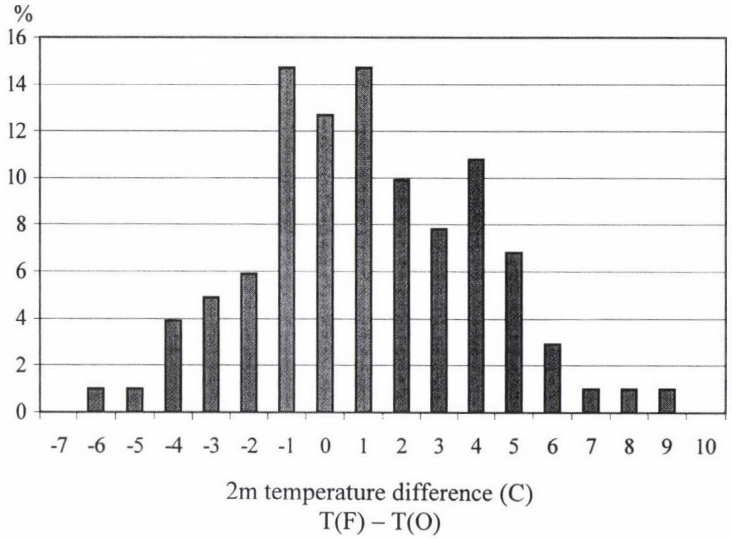

(e)

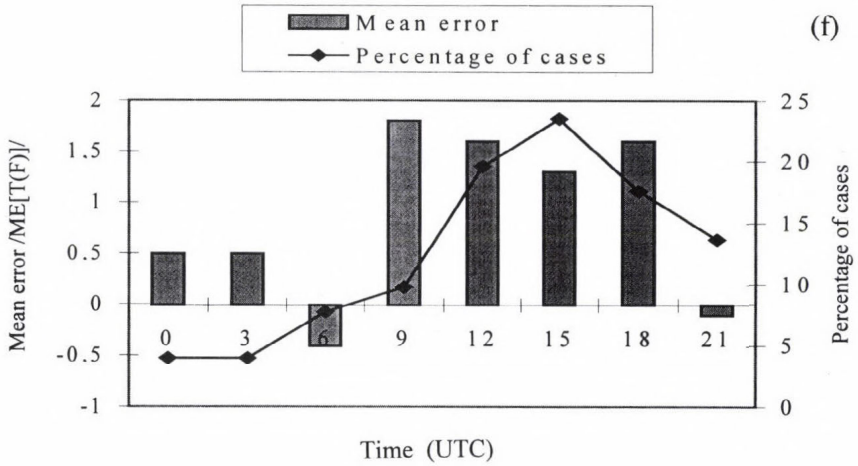

(f)

4.3.4 Forecast of 2m temperature [T(F)]

It is well known in the practice of making very short range forecasts for the region of Lake Balaton that the forecasts according to ALADIN/HU meteograms of 2m temperature are significantly overestimated. That is why it was necessary to use some correction for these data. Statistically we did not find any difference between the results belonging to the two local points (Siófok, Keszthely). The mean forecast error [ME/T(F)/] was +1.09°C with

standard deviation of 2.93°C. The results are shown in *Fig. 9e*. It is worth considering the distribution in time (every 3 hours) of mean forecast errors according to ALADIN/HU for 2m temperature. As it can be seen on *Fig. 9f,* the significant overestimation appears between 09 and 18 UTC, which period is most important for the holiday-makers near Lake Balaton.

5. Concluding remarks

On the basis of the simulation experiments of the two selected squall lines, it can be underlined that the ALADIN model is able (even in operational version) to simulate a squall line although with deficiencies. It seems that the modification of available humidity for convection and the introduction of downdraft brings some benefits for the forecasting practice. So the ALADIN model is a useful tool for the storm forecasters at Lake Balaton. Since the quality of the forecast depends on the weather situation, we can use the following procedure:

The unstable periods are marked out monitoring continuously the forecasts made in 1- or 3-hour steps according to the ALADIN/HU meteograms for the two local points of Lake Balaton on the basis of data sources at 00 and 12 UTC. When the reality of ALADIN/HU forecasts is supported by the actual meso-analyses on the surface and the relevant analyses on the higher pressure levels, we can use the convection parameter tuning similar to our experiments for forecasting the development in space and time of organised convection considering the unstable period marked out.

Nevertheless, more experiments are necessary to evaluate the impact of the new modifications regarding the convection parameterization.

The values of accuracy for the forecasts of ALADIN model can be corrected by considering the quicker (e.g., daily or weekly) change of water temperature at Lake Balaton than it appears in the monthly climatic averages. The systematic errors of 2m temperature and 10m wind velocity forecasts according to ALADIN/HU meteograms can be corrected by filtering (e.g., Kalman-filter) procedure.

The model output data can be used for the nowcasting decision-making procedure (Fig. 1) of storm warning at Lake Balaton as input data, after correcting the forecasts for temperature and wind velocity of ALADIN/HU meteograms. This procedure provides a more objective foundation for storm warnings at Lake Balaton.

Acknowledgements—The authors are grateful to all the members of the ALADIN project, especially to *Jean-François Geleyn* as the project leader, and to *Doina Banciu* for their personal guidance and comments provided in Toulouse.

References

Banciu, D. and *Geleyn, J.-F.*, 1998: Les effets l'introduction de la parametrization des courants descendants convectifs dans le modele atmospherique ALADIN. *Atelier de Modélisation de l'Atmosphere*, 8-9 decembre 1998, Toulouse, 70-73.

Bartha, I., 1987: An objective decision procedure for prediction of maximum wind gusts associated with Cumulonimbus clouds. *Időjárás 91*, 330-346.

Bartha, I., 1998: ALADIN model from the storm forecaster point of view. *Internal Report on the experiments made in Toulouse during 19/10/1998 - 19/12/1998.* Manuscript.

Bartha, I., Gyarmati, Gy., Horváth, Á., Lénárt, L. and *Nagy, J.*, 1998: Prediction of wind storms associated convective activity using radar data (in Hungarian). *Meteorological Notes of Universities 11*, 89-93, Budapest.

Bougeault, Ph., 1985: A simple parameterization of the large-scale effects of Cumulus convection. *Mon. Wea. Rev. 113*, 2108-2121.

Ducrocq, V. and *Bougeault, P.*, 1995: Simulation of an observed squall line with a meso-beta scale hydrostatic model. *Weather and Forecasting*, 380-399.

Fawbush, E. J. and *Miller, R. C.*, 1954: A basis for forecasting peak wind gusts in non-frontal thunderstorms. *Bull. Amer. Meteorol. Soc. 5*, 1.

Gerard, L., 1998: Paramétrisation du profil de quantité de mouvement horizontale dans le nuage convectif. *Atelier de Modélisation de l'Atmosphére*, 8-9 decembre 1998, Toulouse, 74-77.

Gregory, D., Kershaw, R. and *Innes, P. M.*, 1997: Parameterization of momentum transport by convection. II: Tests in single-column and general circulation models. *Quart. J. Roy. Meteorol. Soc. 123*, 1153-1183.

Horányi, A., Ihász, I. and *Radnóti, G.*, 1996: ARPEGE/ALADIN: A numerical weather prediction model for Central-Europe with the participation of the Hungarian Meteorological Service. *Időjárás 100*, 277-301.

Horváth, Á., Duska, G., Kertész, S. and *Lénárt, L.*, 1998: The HAWK meteorological workstation (in Hungarian). *Légkör XLIII*, 18-23.

Kershaw, R. and *Gregory, D.*, 1997: Parameterization of momentum transport by convection. I: Theory and cloud modelling results. *Quart. J. Roy. Meteorol. Soc. 123*, 1133-1150.

IDŐJÁRÁS

Quarterly Journal of the Hungarian Meteorological Service
Vol. 104, No. 4, October–December 2000, pp. 241–252

Nowcasting of precipitation type Part I: Winter precipitation

István Geresdi[1] and **Ákos Horváth**[2]

[1]*University of Pécs, Institute of Geography,*
H-7624 Pécs, Ifjúság u. 6, Hugary; E-mail: geresdi@ttk.pte.hu

[2]*Hungarian Meteorological Service, Storm Warning Observatory,*
H-8600 Siófok, Vitorlás u. 17, Hungary; E-mail: horvath.a@met.hu

(Manuscript submitted for publication 2 June 2000; in final form 10 October 2000)

Abstract—The purpose of this research was to develop a numerical model to give the type and phase of winter precipitation in real time with high horizontal resolution. This model is a part of the nowcasting system developed by the Hungarian Meteorological Service (HMS). The input data are temperature and water vapor profile with horizontal resolution of 3 km. Melting and refreezing rate of precipitation particles are calculated by a microphysical model. The possible outputs are snow, snow and rain, rain, freezing drizzle and rain, freezing rain, ice pellet. The microphysical model was tested by comparison of the simulated precipitation events with the precipitation types observed at a meteorological station. The input data used for the test were from sounding taken at the same station. Although in some cases the calculation misses the precipitation type and/or phase, generally the categories provided by the simulation agree well with the surface observations. An output given by the nowcasting system and its comparison with ground base observation is also presented.

Key-words: nowcasting, winter precipitation, freezing rain, microphysics, numerical simulation.

1. Introduction

The HMS runs a project to develop a nowcasting system. One of the purposes of this project is to improve the nowcast of form and phase of precipitation. In this paper the method applied for winter cases is presented, and in the second part of this series the technique for estimation of the maximum hail size is intended to publish. Nowcasting of precipitation type during winter in the Carpatian Basin is a very important problem, because of the peculiar geographical

conditions, the appearance of dangerous precipitation type like freezing rain has a relatively high frequency.

Numerous papers have been presented discussing the formation of winter precipitation (e.g., *Rauber et al.*, 1994; *Stweart* and *King*, 1987a, b; *Zerr*, 1995, 1997). These researches have investigated the environmental condition necessary for the formation of freezing rain or melting of snow flakes. Zerr made microphysical calculation to trace the phase change of the falling hydrometeor (*Zerr*, 1997). Our microphysics is very similar to that of presented by *Zerr* (1997), but the effect of evaporation cooling was also taken into consideration. According to *Mitra et al.* (1990) subsaturated conditions can significantly increase the distance needed for completely melting of the ice particles. Correct simulation of the phase change needs detailed microphysical description and good time and spatial resolution of the environmental parameters (temperature and vapor content) in the boundary layer. This could be the reason that — to knowledge of the authors — only case studies were made in this field. This is the first effort which tries to give the phase and type of the precipitation on the ground in real time and with high horizontal resolution. Winter precipitation is divided into six categories: (i) snow, (ii) snow and rain, (iii) rain, (iv) freezing drizzle and rain, (v) freezing rain and (vi) ice pellet.

2. *Description of the model*

Input data of the model are coming from of the nowcasting system developed at the Hungarian Meteorological Service. This system uses real time data of surface observations (SYNOP), forecasted fields of a limited area model ALADIN (*Horányi et al.*, 1996) and calculates the objective analysis using optimal interpolation for data assimilation. Procedure for analysis of relative humidity using radar reflectivity data is also involved. The MEANDER (Mesoscale Analysis Nowcasting and Decision Routines) system produces high resolution (dx, dy $\sim$ 3 km, dz $\sim$ 200 m) 3D fields of basic parameters: pressure, height, temperature, relative humidity and wind.

A low density particle starts to fall with its terminal velocity at the highest 0°C level (denoted by h_0 in *Fig. 1*). Density and type of the particle are very uncertain. They strongly depend on the microphysical processes taken place in the cloud. In this research the particles were supposed to be graupel ones with initial density of 400 kg m^{-3}. Previous laboratory results show that the meltwater does not shed and remains attached to the ice core if the diameter of the graupel particle is less than 9 mm (*Rasmussen et al.*, 1984). These observations support the assumption that the mass of the falling hydrometeor changes only due to the diffusional transport of water vapor. The equations suggested by *Rasmussen* and *Heymsfield* (1987) were used to calculate the terminal velocity

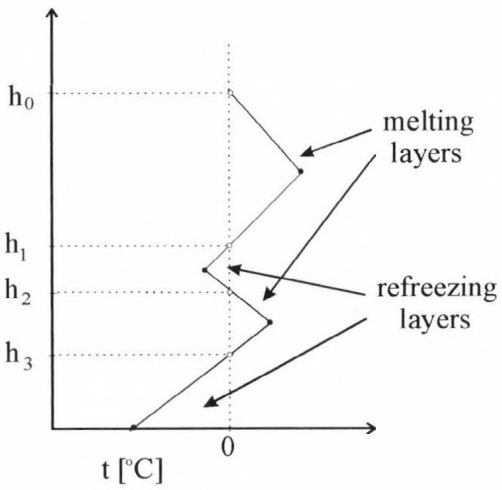

Fig. 1. Main characteristics of a temperature profile used as the model input. While the values at the significant levels (black dots) are given by another subprogram, the height of 0°C levels are calculated in the model.

of the falling particle. It is supposed that the falling particle does not collect either liquid or solid hydrometeors. So the heat transfer from the collected particles could be neglected, and the melting rate depends only on the heat transfer from the ambient air and the heat released due to the diffusion of water vapor from the surface of the particle:

$$\frac{dm_i}{dt} = \frac{1}{L_f} \cdot \frac{dq}{dt}, \tag{1}$$

where m_i and L_f are the mass of the ice core and the latent heat of fusion, respectively. The heating rate is given by the next equation:

$$\frac{dq}{dt} = C \cdot \left\{ -4\pi \cdot r_g \cdot k_a \cdot (T_\infty - T_s) \cdot f_h - 4\pi \cdot r_g \cdot L \cdot D_v \cdot (\rho_{v,\infty} - \rho_{v,s}) \cdot f_v \right\}, \tag{2}$$

where C depends on the Reynolds number (*Rasmussen* and *Heymsfield,* 1987). If $N_{Re} < 250$ C is equal to 2, otherwise C is unit. r_g is the radius of the particle, k_a and D_v are heat conductivity of air and vapor diffusion coefficient in air, respectively (*Pruppacher* and *Klett*, 1997). T_∞ and T_s are the temperature in the environment and on the surface of the graupel, $\rho_{v,\infty}$ and $\rho_{v,s}$ are the va-

por density far from the graupel and on its surface. L is the latent heat of condensation if the graupel is completely or partly melted, otherwise it means the latent heat of deposition. f_v and f_h are ventilation coefficients for vapor and heat transfer (*Pruppacher* and *Klett*, 1997), respectively:

$$f_v = 0.78 + 0.308 \cdot N_{Sc}^{1/3} \cdot N_{Re}^{1/2},$$

$$f_h = 0.78 + 0.308 \cdot N_{Pr}^{1/3} \cdot N_{Re}^{1/2},$$

where N_{Sc} and N_{Pr} are the Schmidt and Prandtl numbers. The first term between the brackets in Eq. (2) is the heat transfer due to the conduction, the second term is the releasing latent heat due to vapor diffusion.

When an incompletely melted particle falls into the refreezing layer (Fig. 1), the ice core starts to increase. The rate of the increase is given by the following equations (*Johnson* and *Hallett*, 1968):

$$\frac{dy}{dt} = -\frac{1}{3 \cdot y^2 \cdot t_0}, \tag{3}$$

where

$$t_0 = \frac{\rho_w \cdot L_f \cdot r_g^2}{3 \cdot f_h \cdot k_a \cdot \Delta T}\left(1 - \frac{\Delta T \cdot c_w}{L_f}\right),$$

and

$$y = \frac{a}{r_g},$$

where r_g is the radius of the melted particle and a is the radius of the ice core. ρ_w, L_f, and c_w are the density of water, the latent heat of fusion and the specific heat of water, respectively. ΔT is the supercooling of the water ($\Delta T = 273.15 - T_s$). Relatively small time step of 1 s was used during the calculation to avoid overestimation heat transfer.

To give the type of the particles on the ground, the critical radius (R_{crit}) is calculated at every grid point where existence of precipitation was detected by radar. The meaning of the critical size is that the particles are completely melted if their initial size is smaller than the critical size. Graupel particles with larger size remain frozen or have an ice core when they reach the ground. The initial radius is calculated by the following recursive formulas:

$$R_n = 0.5 \cdot R_{n-1}$$

if the particle with initial radius of R_{n-1} did not melt completely, and

$$R_n = 0.5 \cdot (R_{n-2} + R_{n-1})$$

if the particle with initial radius of R_{n-1} completely melted, but the one with that of R_{n-2} did not. R_0 was chosen to be 3 mm. The calculation was ceased when $|R_n - R_{n-1}| < 0.1$ mm and $R_{crit} = R_n$. One of the six categories for the precipitation type was chosen depending on the value of R_{crit}, surface temperature and number of the melting layer (*Fig. 2*). Specification of precipitation type was based on the relation between R_{crit} and a given radius (R^*). R^* was related to the size distribution of the graupel particles in the cloud. It was supposed that the concentration of the particles larger than R^* is negligible. In this research R^* was chosen to be a constant value of 1.0 mm. In most cases this value is acceptable, concentration of the garupel particles larger than 2.0 mm is very low in layer clouds (solid line in *Fig. 3*). If R_{crit} is larger than R^* most of the precipitable particles melt, and depending on the surface temperature the precipitation on the ground is freezing rain or rain. If R_{crit} is less than 0.1 mm, only few liquid particles can fall on the ground, because water drops smaller than 0.1 mm generally evaporate before reaching the ground. In this case the precipitation is ice pellet or snow. If R_{crit} is between R^* and 0.1 mm the precipitation is mixed type: snow and rain if the ground temperature is over 0°C, and ice pellet and freezing drizzle otherwise.

Of course R_{crit} is not calculated when the maximum temperature is below the melting temperature in the air mass above the grid point. In this case the model output is snowfall.

3. Evaluation of the microphysical model

The model was tested by comparison of calculated and observed data. The test focused mainly on the formation of the freezing rain. Freezing rain or drizzle can produce extremely dangerous conditions for almost every kind of traffic by coating the surface with continuous ice layer. Precipitation type reported from synoptic station located in Budapest was compared with calculated data (*Table 1*). The temperature profiles were given from data measured by rawinsondes taken two times a day (12:00 UTC and 00:00 UTC) from this station. Sounding data, nearer to the beginning of precipitation events were used to give ambient conditions for the falling particles. The observed precipitation type is given in the second column, the value of the critical radius and the simulated precipitation type are written in the third and fourth column, respec-

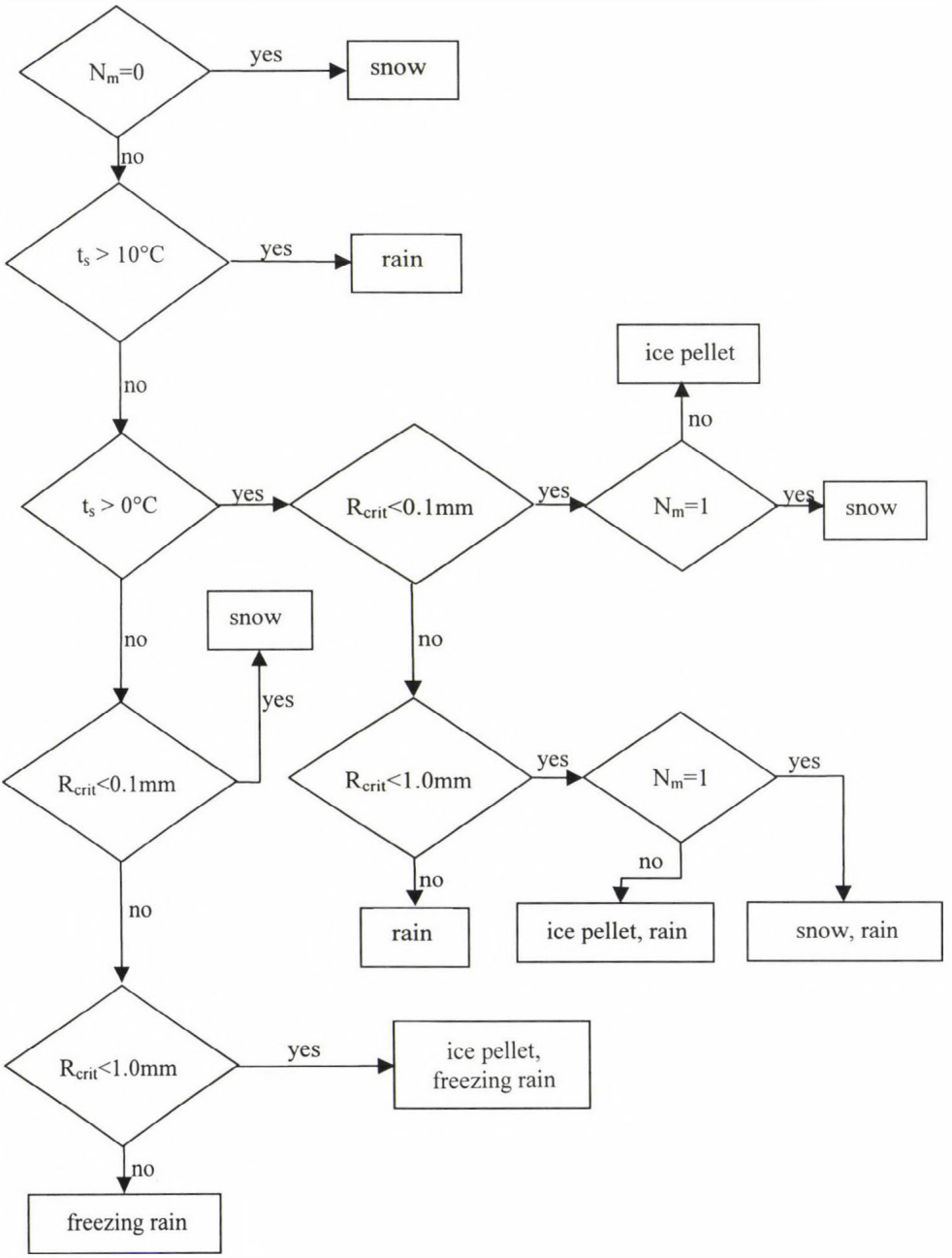

Fig. 2. Flow chart used to separate the different precipitation types. The decision depends on the number of the melting level (N_m), the surface temperature (t_s) and the value of the critical radius (R_{crit}). More details about R_{crit} are in the text.

tively. Between 1991 and 1997 one or more melting layers were observed on 41 days. In this period freezing rain was reported on 21 days. Six other days — when other precipitation types were also observed — were also involved into the dataset. Because the calculation confined to the lowest, 2–3 km thick air layer, sounding data describe well the environmental condition for the falling particles, if short time passes between the sounding and the precipitation fall out. Fortunately the time gap between the sounding and the report of the precipitation was longer than 4 h only in few cases.

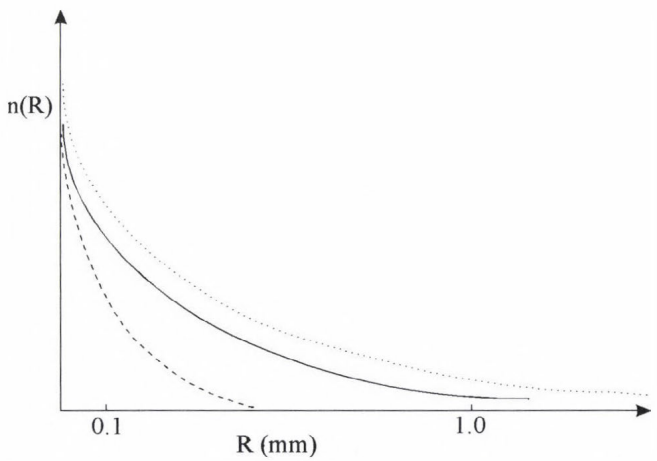

Fig. 3. Dependence of the size distribution on the precipitation intensity. At present calculation it was supposed that the size distribution of the garupel particles is given by thick solid line. If the precipitation intensity increases number concentration of particles larger than 1 mm increases (dotted line). If the precipitation intensity decreases the maximum particle radii is smaller than 1 mm (dashed line).

Comparison of data in the third and fourth column shows that the observed and the simulated precipitation types agree well. However, the model was not able to describe the change of the precipitation type between two soundings. This is not necessarily caused by change of the temperature profile. The fluctuation in precipitation intensity can result in similar effect. If the intensity decreases, the number concentration of the larger particles also decreases (dashed line in Fig. 3). In this case $R_{crit} < 1.0$ mm does not mean that some of the particles will have an ice core on the ground, but all of them will completely melt. Because $R^* = 1.0$ mm is used to separate the different precipitation types, the model prefers the formation of ice pellet and freezing rain to the freezing rain, furthermore it overestimates the occurrence of snow and

Table 1. Comparison of the observed and calculated precipitation type. Observation times are given in UTC. Rows shaded by gray show the days when the difference between the observation and simulation were significant

Date	Duration	Observed precip.	R_{crit} (mm)	Simulated precipitation
12. 20. 1991	10:25 - 11:00	ice pellet	0.21	ice pellet, snow
	11:00 - 11:10	ice pellet	0.21	ice pellet, snow
12. 29. 1991	21:15 - 21:50	ice pellet	0.25	ice pellet, snow
01. 05. 1992	08:30 - 09:00	freezing rain	1.5	freezing rain
01.28. 1992	01:00 - 04:00	freezing drizzle	-	snow
12. 21. 1992	08:05 - 10:10	freezing rain	0.70	ice pellet, freezing rain
	10:10 - 10:50	ice pellet	0.70	ice pellet, freezing rain
	10:50 - 12:20	freezing rain	0.70	ice pellet, freezing rain
	20:20 - 20:50	ice pellet	0.70	ice pellet, freezing rain
	20:50 - 21:00	freezing rain	0.70	ice pellet, freezing rain
01. 06. 1993	20:30 - 21:00	ice pellet	0.66	ice pellet, freezing rain
01. 07. 1993	09:30 - 10:20	freezing rain	1.38	freezing rain
	11:20 - 15:00	freezing rain	1.38	freezing rain
01. 08. 1993	16:40 - 17:30	freezing rain	1.75	freezing rain
	17:30 - 19:10	freezing drizzle	1.75	freezing rain
02. 06. 1993	11:35 - 14:00	freezing rain	0.88	ice pellet, freezing rain
	14:30 - 15:00	freezing rain	0.88	ice pellet, freezing rain
	18:30 - 19:00	ice pellet	0.88	ice pellet, freezing rain
12. 28. 1993	07:15 - 08:00	ice pellet	0.87	ice pellet, rain
01. 23. 1994	21:35 - 23:40	freezing rain	1.48	freezing rain
12. 05. 1994	01:20 - 04:00	freezing drizzle	2.00	freezing rain
12. 28. 1994	05:00 - 09:00	freezing rain	1.85	freezing rain
01. 22. 1995	evening	freezing rain	2.23	freezing rain
11. 24. 1995	05:20 - 06:30	snow	-	snow
	06:30 - 09:00	freezing drizzle	0.47	ice pellet, freezing rain
	09:00 - 24:00	snow	0.47	ice pellet , freezing rain
11. 25. 1995	00:00 - 06:30	snow	0.93	ice pellet, freezing rain
12. 18. 1995	01:25 - 04:55	freezing rain	1.2	freezing rain
	04:55 - 08:00	freezing drizzle	1.2	freezing rain
12. 20. 1995	20:15 - 21:20	snow and rain	0.83	snow and rain
	21:20 - 23:00	rain	0.83	snow and rain
12. 31. 1995	20:10 - 22:55	freezing rain	-	snow
01. 07. 1996	13:40 -14:10	freezing rain	0.34	ice pellet, freezing rain
	14:10 -15:10	ice pellet	0.34	ice pellet, freezing rain
	16:40 -20:20	freezing rain	0.34	ice pellet, freezing rain
01. 08. 1996	01:10 -02:15	freezing rain	1.00	freezing rain
01. 26. 1996	03:00 - 05:30	freezing drizzle		snow
	09:10 - 09:30	ice pellet		snow
	11:30 - 12:00	ice pellet		snow
	17:20 - 20:00	freezing drizzle		snow
	23:35 - 02:15	freezing rain	0.64	ice pellet, freezing rain
01. 27. 1996	07:15 - 09:00	freezing rain	0.64	ice pellet, freezing rain
02. 03. 1996	05:40 - 08:10	freezing rain	0.28	ice pellet, freezing rain
01. 03. 1997	08:45 - 11:40	freezing rain	0.12	ice pellet, freezing rain
	11:40 - 12:40	ice pellet	0.12	ice pellet, freezing rain
	12:40 - 13:00	freezing rain	0.12	ice pellet, freezing rain
	13:00 - 14:00	ice pellet	0.12	ice pellet, freezing rain
	14:00- 23:20	freezing rain	0.89	ice pellet, freezing rain
01. 04. 1997	05:09 -05:40	freezing rain	0.89	ice pellet, freezing rain
12. 19. 1997	11:06 - 12:00	ice pellet	0.85	ice pellet, freezing rain
	12:00 - 12:20	freezing rain	0.85	ice pellet, freezing rain

rain against only rain. When the precipitation intensity increases, the number concentration of the particles at the tail of the size distribution also increases (dotted line in Fig. 3). More graupel particles can survive the fall through the melting layer than it could be expected from the model results. The appearance of larger particles increases the possibility of the ice pellet events against the freezing rain ones. The problem caused by the fluctuation of precipitation intensity could be solved by linking the value of R^* to the radar reflectivity, instead of using fixed value.

Within the investigated period the model was not able to predict correctly the precipitation types on five days.

(a) On January 28, 1992, although freezing drizzle was reported between 01:00 and 04:00 UTC, the model output was snow. Analysis of the sounding data shows that just before the precipitation started to fall, temperature was below 0°C (the maximum temperature was equal to -3°C and measured on the surface), and the presence of the melting layer was indicated only 24 hours later by next midnight sounding. It is assumed that this freezing drizzle event did not originate from ice clouds. If the cloud top temperature is larger than -10°C, only few ice crystals can form and the collision-coalescence of the supercooled droplets results in drizzle size drops ($>50\mu m$). If the cloud base is near to the ground, these small drops can reach the ground.

Freezing drizzle event occurred also on December 31, 1995, and it could be the consequence of similar microphysical processes, because no melting layer was observed this day as well.

(b) On November 24, 1995, snowfall started early in the morning at 5:20 UTC and it ended only in the next morning. This continuous snowfall was interrupted by freezing drizzle events occurred between 6:30 UTC and 9:00 UTC. The model simulated well the precipitation types until 9:00. While the surface observer reported snow from 9:00, the model output did not change, it remained ice pellet and freezing rain. The sounding taken at 12:00 UTC and 00:00 UTC on November 25 indicated a melting layer. The characteristic parameters of the melting layer — depth and the maximum temperature — increased form 600 m to 800 m and from 0.8°C to 2.0°C, respectively. This strong warming resulted in favorable condition for freezing rain formation and some of the particles should have melted. It is assumed that observation error caused the discrepancy in this case.

(c) The differences between observed and simulated precipitation types on January 26, 1996, were caused by different reasons. The freezing drizzle events at dawn (3:00–5:30 UTC) could be the consequence of the formation of supercooled drops, because melting layer was not observed neither

at 00:00 UTC nor at 12:00 UTC soundings (see point (a)). Unfortunately the model is not able to simulate the formation of large supercooled drops via collision–coalescence processes of small water drops. This is the reason of that the model gave snow instead of freezing drizzle. After 9:00 the observed precipitation type was ice pellet and the model output was snow. Due to the absence of melting layer, melting and subsequent refreezing could not occur. It is assumed that this discrepancy was caused by observational uncertainty. The midnight sounding indicated melting layer and the model results agrees well with the observation after 23:15 UTC. The difference noticed in the time interval of 17:20–20:00 UTC could be caused by change of the ambient conditions. The model used the environmental parameters given by 12:00 UTC sounding, which were not consistent with environmental condition at late afternoon. Although the time difference between the precipitation events and the 00:00 UTC sounding (on 27 January) was large, it might have been more suitable to use.

4. Application

The above described microphysical model is in operative usage at the Hungarian Meteorological Service as a part of the MEANDER system. In every grid point a radar reflectivity value is provided, which represents the radar measured precipitation intensity of the given area. The precipitation type decision model runs only in grid points where radar echoes indicate precipitation, saving considerable run time. Distribution of precipitation phase can be displayed on the operative meteorological workstation among other derived meteorological image type information.

Fig. 4 shows the output of the system on 24 November, 1999. Early in the morning of this day precipitation types were freezing rain and snow. Cloud formation was initiated by a warm advection at the middle tropospheric level in the warm sector of a Mediterranean cyclone. Since temperature remained below 0°C on the surface, conditions were favorable for freezing rain formation. On areas where the warm advection had resulted in melting layer, freezing rain event occurred, elsewhere the form of precipitation was snow. Dark gray regions denote freezing rain events and white regions denote the snowfall. For comparison with surface observation, the observed precipitation types reported by the meteorological stations are also given in the figure. The calculated precipitation type agrees well with the observation in Transdanubia region, but there are some discrepancies in the southeastern and the northeastern part of the country. The limited area model might have overestimated the warm advection over the northeastern region and might have underestimated the increase of temperature over the southeastern region.

Although the model simulates well the precipitation types in most cases, improvements are planned. To take into account the possible effect of change of precipitation intensity, the value of R^* will be calculated on the base of radar reflectivity data.

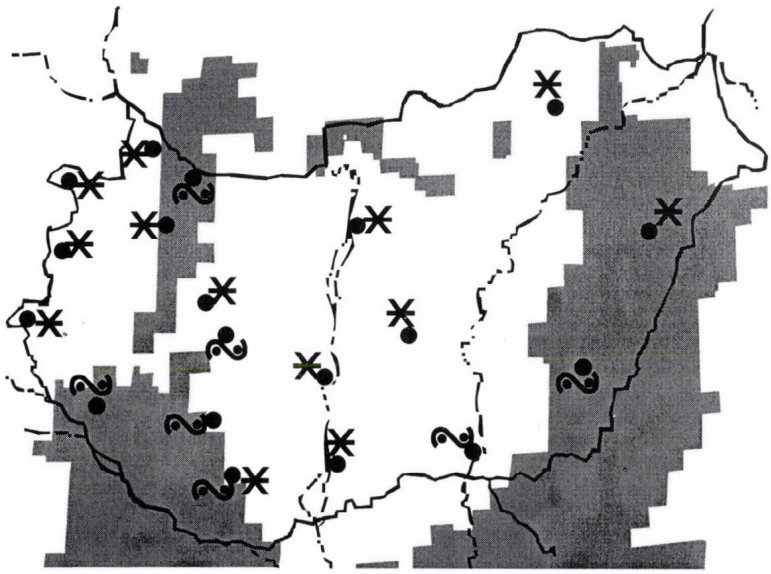

Fig. 4. Nowcasting system output for winter precipitation type at 9:00 UTC on November 24, 1999. The dark gray and white regions denote the freezing rain events and snow fall, respectively. Also the precipitation types reported between 6:00 and 9:00 UTC by meteorological stations (black dots) are shown. Symbol ∿ and * denote freezing rain and snowfall, respectively.

Test data suggest that a few percent of freezing drizzle events occurred without melting layer. Unfortunately the model with simple microphysics is not able to describe the formation of large supercooled drops. The uncertainty both in form and value of initial density of the falling particles can effect the final result. The authors think that the application of the polarized radar data can help to solve these problems and the data given by this type of radar are intended to use in future.

Acknowledgement—The research was supported by the Hungarian Scientific Research Fund (Number: T030857).

References

Horányi, A., Ihász, I. and *Radnóti, G.*, 1996: ARPAGE/ALADIN: A numerical weather prediction model for Central-Europe with the participitation of the Hungarian Meteorological Service. *Időjárás 100,* 277-301.

Johnson, D. A. and *Hallett, J.*, 1968: Freezing and shattering of the supercooled water drops. *Quart. J. Roy. Meteorol. Soc. 94,* 468-482.

Mitra, S. K., Vohl, O., Ahr, M. and *Pruppacher, H. R.*, 1990: A wind tunnel and theoretical study of the melting behavior of atmospheric ice particles. IV: Experiment and theory for snow flakes. *J. Atmos. Sci. 47,* 584-591.

Pruppacher, H. R. and *Klett, J. D.*, 1997: *Microphysics of Clouds and Precipitation.* Kluwer Academic Publisher, p. 954.

Rasmussen, R. M. and *Heymsfield, A. J.*, 1987: Melting and shedding of graupel and hail. Part I: Model physics. *J. Atmos. Sci. 44,* 2754-2763.

Rasmussen, R. M., Levizzani, V. and *Pruppacher, H. R.*, 1984: A Wind Tunnel and Theoretical Study on the Melting Behavior of Atmospheric Ice Particles: III. Experiment and Theory for Spherical Ice Particles of Radius < 500 μm. *J. Atmos. Sci. 41,* 381-388.

Rauber R. M., Ramamurthy, M. K. and *Tokay, A.*, 1994: Synoptic and mesoscale structure of a severe freezing rain event: The St. Valentine's Day ice storm. *Wea. Forecasting 9,* 183-208.

Stewart, R. E. and *King, P.*, 1987a: Freezing precipitation in winter storms. *Mon. Wea. Rev. 115,* 1270-1279.

Stewart, R. E. and *King, P.*, 1987b:Rain-snow boundaries over southern Ontario. *Mon. Wea. Rev., 115,* 1894-1907.

Zerr, R. J., 1995: Wind and reflectivity signatures as obtained by a Doppler radar for a freezing-rain episode. *Preprints, 27th Conf. On Radar Meteorology,* Vail, Co. *Amer. Meteorol. Soc.,* 414-415.

Zerr, R. J., 1997: *Freezing rain: An observational and theoretical study. J. Appl. Meteorol. 36,* 1647-1661.

IDŐJÁRÁS

Quarterly Journal of the Hungarian Meteorological Service
Vol. 104, No. 4, October–December 2000, pp. 253–268

Urban heat island development affected by urban surface factors

János Unger[1], Zsolt Bottyán[2], Zoltán Sümeghy[1] and Ágnes Gulyás[1]

[1]Department of Climatology and Landscape Ecology, University of Szeged, P.O. Box 653, H-6701 Szeged, Hungary; E-mail: unger@geo.u-szeged.hu, sumeghy@geo.u-szeged.hu, agulyas@geo.u-szeged.hu
[2]Department of Natural Sciences, Zrínyi University, P.O. Box 1, H-5008 Szolnok, Hungary; E-mail: zbottyan@solyom.szrfk.hu

(Manuscript submitted for publication 8 May 2000; in final form 11 September 2000)

Abstract—This study examines the spatial and quantitative influence of urban factors on the surface air temperature field of the medium-sized city of Szeged, Hungary, using of mobile measurements under different weather conditions between March 1999 and February 2000. This city with a population of about 160,000 is situated on a low, flat flood plain. The efforts have been concentrated on investigating the development of the urban heat island (UHI) in its peak development during the diurnal cycle. Tasks include determination of spatial distribution of mean maximum UHI intensity, using of standard kriging procedure and determination of statistical model equations in the one-year study period, as well as in the heating and non-heating seasons. Multiple correlation and regression analyses are used to examine the effects of urban surface parameters (land-use characteristics and distance from the city centre determined in a grid network) on the UHI. Results indicate isotherms increasing in regular concentric shapes from the suburbs toward the inner urban areas with a seasonal variation in the UHI magnitude. In the city centre the mean maximum UHI intensity reaches more than 2.6°C, 3.1°C and 2.1°C, respectively. As the patterns show, there is a clear connection between urban thermal excess and built-up density. As the model equations show, strong relationships exist between urban thermal excess and distance, as well as built-up ratio, but the role of water surface is negligible.

Key-words: UHI, spatial distribution, grid network, built-up ratio, water surface ratio, distance, statistical analysis, regression equations.

1. Introduction

The temperature-increasing effect of cities caused by urbanization (the so-called urban heat island — UHI) is one of the most deeply examined fields of climatology. Features of the UHI are well documented from different cities mainly from the temperate zone (e.g., *Oke*, 1997; *Kuttler*, 1998) and one of

the most difficult aspect of this phenomenon is studying of its peak development during the diurnal cycle.

The detection of real factors and physical processes generating the distinguished urban climate is extremely difficult because of the very complicated urban terrain (as regard surface geometry and materials) as well as artificial production of heat and air pollution. The simulation of these factors and processes demands complex expensive instrumentation and sophisticated numerical and physical models. Despite these difficulties, several models have been developed for studying small-scale climate variations within the city, including the ones based on energy balance (*Tapper et al.*, 1981; *Johnson et al.*, 1991; *Myrup et al.*, 1993), radiation (*Voogt* and *Oke*, 1991), heat storage (*Grimmond et al.*, 1991), water balance (*Grimmond* and *Oke*, 1991) and advective (*Oke*, 1976) approaches.

As an other solution of the above mentioned problems, utilisation of statistical models may provide useful tools, which give us quantitative information about the magnitude as well as spatial and temporal features of the UHI intensity (defined as the temperature difference between urban and rural areas) by employing urban and meteorological parameters. Some examples of the modeled variables (surface and near surface air UHI intensity or even the possible maximum UHI intensity) and the employed variable parameters are gathered in *Table 1*.

Table 1. Survey of some statistical models with modeled UHI variables, employed parameters and authors

Modeled variable	Employed parameters	Author(s)
UHI intensity	wind speed, cloudiness	*Sundborg* (1950)
UHI intensity	population, wind speed	*Oke* (1973)
Max. UHI intensity	population	
UHI intensity	wind speed, wind speed, cloudiness, atmospheric stability, traffic flow, energy consumption, temperature	*Nkemdirim* (1978)
UHI intensity	wind speed, land-use type ratios	*Park* (1986)
Max. UHI intensity	impermeable surface, population	
UHI intensity	cloudiness, wind speed, temperature, humidity mixing ratio	*Goldreich* (1992)
Surface UHI intensity	solar radiation, wind speed, cloudiness	*Chow et al.* (1994)
UHI intensity	built-up area, height, wind speed, time, temperature amplitude	*Kuttler et al.* (1996)

Counting all weather conditions except rain, the main purpose of this study is to investigate the effects and interactions inside the city on the surface air temperature a few hours after sunset, when the UHI effect is most pro-

nounced. To achieve this aim, we construct horizontal isotherm maps to show the average spatial distribution of maximum UHI intensity in the investigated period as a whole and in the distinguished, so-called heating and non-heating, seasons. Then, we intend to reveal some obvious relationships between temperature patterns and urban factors using built-up (covered surface) ratio within the city. Further aim was to determine quantitative influences of the urban surface factors on the patterns of urban-rural temperature.

2. Study area and methods

Szeged is located in the south-eastern part of Hungary on the Great Hungarian Plain (46°N, 20°E) at 79 m above sea level (*Fig. 1*). The city and its countryside situate on is a large flat flood plain. The River Tisza passes through the city, otherwise, there are no large water bodies nearby. This geographical situation (no orographic climate influences) makes Szeged a good case for the study of a relatively undisturbed urban climate. Using Köppen's classification, the area belongs to the climatic region *Cf*, which means a temperate warm climate with a rather uniform annual distribution of precipitation (*Table 2*). The regional climate of Szeged has, however, a certain Mediterranean influence. It appears mainly in the annual variation of precipitation, namely in every 10 years approximately 3 years show some Mediterranean (relatively high autumn-winter rainfall) characteristics (*Unger*, 1999).

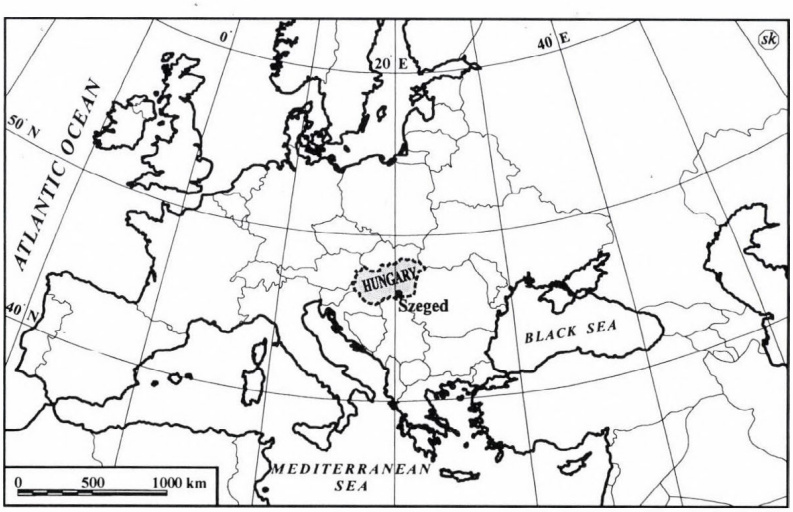

Fig. 1. Location of Hungary and Szeged in Europe.

Table 2. Monthly and annual means or sums of meteorological parameters in the region of Szeged (1961–1990)

Parameter	J	F	M	A	M	J	J	A	S	O	N	D	Year
Temperature (°C)	-1.8	1.0	5.6	11.1	16.2	19.2	20.8	20.2	16.4	11.0	5.1	0.6	10.4
Precipitation (mm)	29	25	29	40	51	72	50	60	34	26	41	40	497
Sunshine duration (h)	62	87	143	181	235	252	288	267	211	170	82	51	2029
Cloudiness (%)	70	68	63	60	58	54	45	42	45	49	69	76	58
Wind speed (ms^{-1})	3.3	3.4	4.0	3.7	3.2	2.9	2.9	2.7	2.6	3.0	3.0	3.7	3.2
Relative humidity (%)	85	82	73	68	66	67	65	67	70	73	83	87	74
Vapor pressure (hPa)	4.9	6.5	6.8	8.9	12.3	15	16	15.8	13.2	9.8	7.6	5.8	10.1

The city's population of 160,000 (1998) lives within an administration district of 281 km^2. As for the city structure, its basis is a boulevard-avenue road system. Numbers of different land-use types are present including a densely built center with medium wide streets and large housing estates of tall concrete blocks of flats set in wide green spaces. Szeged also contains areas used for industry and warehousing, zones occupied by detached houses and considerable open spaces along the banks of the river, in parks and around the city's outskirts (*Fig. 2*).

As the urban and suburban areas occupy only about 25–30 km^2, our investigation focused only on the inner part of the administration district (Fig. 2). This study area was divided into two sectors and subdivided further into 0.5 km × 0.5 km square grid cells (*Fig. 3*). The same grid size was employed, for example, in a human bioclimatological analysis of Freiburg, Germany, a city of similar size to Szeged (*Jendritzky* and *Nübler*, 1981) and in an other investigation of UHI in Seoul, Korea (*Park*, 1986). *Sailor* (1998) chose a 2 km × 2 km network for his hypothetical city, where he simulated the impacts of vegetative augmentation on the annual heating and cooling degree days. Therefore, our grid network can be regarded as a rather dense one. In the study area there are 107 grid cells totaling 26.75 km^2, covering the urban and suburban parts of Szeged (mainly inside of the circle dike that protects the city from floods caused by the Tisza River). Outlying parts of the city, characterized by village and rural features, are not included in the grid except for four cells at the western side of the area. These cells are needed in order to determine the temperature contrast between urban and rural areas. The grid was established by quartering the 1 km × 1 km square network of the Unified

National Mapping System (EOTR), that can be found on topographical maps of Hungary at the scale of 1:10,000.

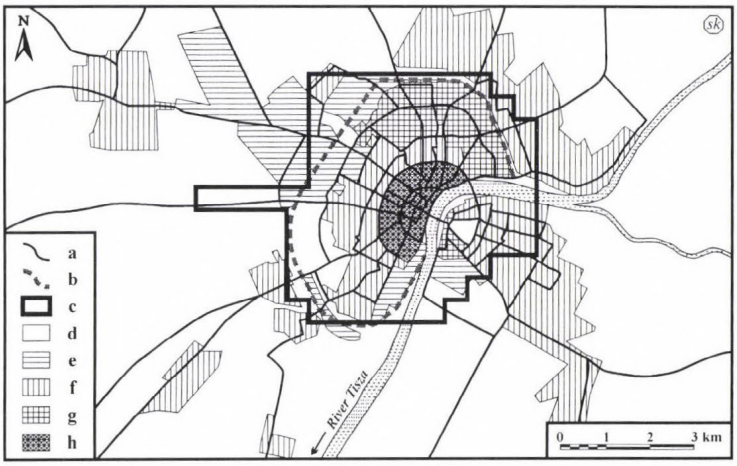

Fig. 2. Characteristic land-use types and road network in Szeged: (**a**) road, (**b**) circle dike, (**c**) border of the study area, (**d**) agricultural and open land, (**e**) industrial area, (**f**) 1–2 storey detached houses, (**g**) 5–11 storey apartment buildings and (**h**) historical city core with 3–5 storey buildings.

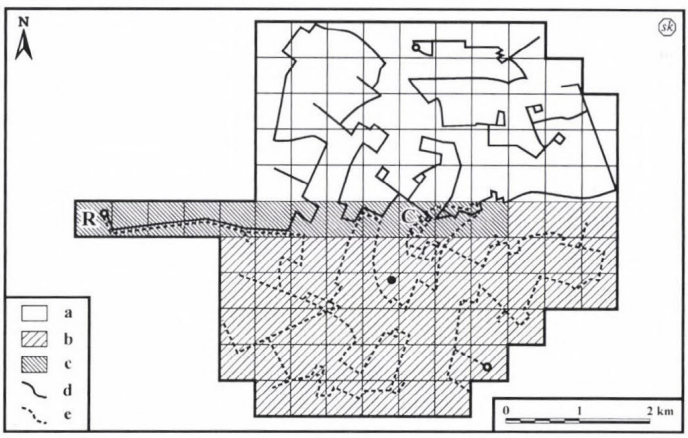

Fig. 3. Division of the study area into 0.5 km × 0.5 km grid cells: (**a**) northern sector, (**b**) southern sector, (**c**) overlap area and (**d, e**) the measurement routes. Rural and central grid cells are indicated by R and C, respectively. The permanent measurement site at the University of Szeged is indicated as •.

The examination of the spatial and temporal distribution of surface air temperature was based on mobile observations during the period of March, 1999–February, 2000. In case of surface UHI and near surface air UHI investigations, the moving observation with different vehicles (car, tram, helicopter, airplane, satellite) is an often used process (e.g., *Johnson*, 1985; *Yamashita*, 1996; *Voogt* and *Oke*, 1997; *Klysik* and *Fortuniak*, 1999; *Tumanov et al.*, 1999).

In order to collect data on maximum UHI intensity (namely the temperature difference between urban and rural areas) at every grid cell, mobile measurements were performed on fixed return routes once a week during the studied period (altogether 48 times) to accomplish an analysis of air temperature over the entire area. This one-week frequency of car traverses secured sufficient information on different weather conditions, except for rain.

Division of the study area into two sectors was needed because of the large number of grid cells. The northern and southern sectors consisted of 59 grid cells (14.75 km^2) and 60 grid cells (15 km^2), respectively, with an overlap of 12 grid cells (3 km^2). The lengths of the fixed return routes were 75 and 68 km in the northern and southern sectors, respectively, and took about 3 hours to traverse (Fig. 3). Such long and return routes were necessary to gather temperature values in every grid cell and to make time-based corrections. Temperature readings were obtained using a radiation-shielded LogIT HiTemp resistance temperature sensor (resolution of 0.01 °C), which was connected to a portable LogIT SL data logger for digital sampling inside the car. Since the data were collected every 16 s at an average car speed of 20–30 km h^{-1} the average distance between measuring points was 89–133 m. The temperature sensor was mounted 0.60 m in front of the car at 1.45 m above ground to avoid engine and exhaust heat. This is similar to the measurement system used by *Ripley et al.* (1996) in Saskatoon, Saskatchewan. The car speed was sufficient to secure adequate ventilation for the sensor to measure the momentary ambient air temperature.

After averaging the measurement values by grid cells, time adjustments to the reference time were applied assuming linear air temperature change with time. This linear change was monitored using the continuous records of the permanent automatic weather station at the University of Szeged (Fig. 3). The linear adjustment appears to be correct for data collected a few hours after sunset in urban areas. However, because of the different time variations of cooling rates, it is only approximately correct for suburban and rural areas (*Oke* and *Maxwell*, 1975). The reference time, namely the likely time of the occurrence of the strongest UHI, was 4 hours after sunset, a value based on earlier measurements in 1998 and 1999 (*Boruzs* and *Nagy*, 1999). Consequently, every grid cell of 59 in the northern sector or every grid cell of 60 in

the southern sector can be characterized by one temperature value for every measuring night. These temperature values refer to the center of each cell.

We determined urban-rural air temperature differences (UHI intensity) by cells referring to the temperature value of the grid cell (the most western cell in the investigated area), where the synoptic weather station of the Hungarian Meteorological Service is located. This grid cell (labeled by R) containing this station was regarded as rural (Fig. 3), because the records of this station were used as rural data in the earlier studies on the urban climate of Szeged (e.g., *Unger*, 1996, 1999). The 107 points (the above mentioned grid cell center-points) cover the urban parts of Szeged and they provide an appropriate basis to interpolate isolines. The isolines, therefore, can show detailed descriptions of thermal field within the city at the time of the strongest effects of urban factors. In order to draw the isotherms, a geostatistical gridding method, the standard kriging procedure was used.

Parameters of land-use for the grid cells were determined by GIS (Geographical Information System) methods combined with remote sensing analysis of SPOT XS images (*Mucsi*, 1996). Vector and raster-based GIS databases were produced in the Applied Geoinformatics Laboratory of the University of Szeged. The digital satellite image was rectified to the EOTR using 1:10 000 scale maps. The nearest-neighbour method of resampling was employed, resulting in a root mean square value of less than 1 pixel. Since the geometric resolution of the image was 20 m × 20 m, small urban units could be assessed independently of their official (larger scale) land-use classification. Normalised Vegetation Index (*NDVI*) was calculated from the pixel values, according to the following equation:

$$NDVI = (IR - R) / (IR + R), \tag{1}$$

where *IR* is the pixel value in the infrared band and *R* is the pixel value in the red band. The range of *NDVI* values is from –1 to +1, indicating the effect of green space in the given spatial unit (*Lillesand* and *Kiefer*, 1987). Built-up, water, vegetated and other surfaces were distinguished according to the *NDVI* value. The spatial distribution of these land-use types of each grid element was calculated using cross-tabulation.

In order to assess the extent of the relationships between the maximum UHI intensity and various urban surface factors, multiple correlation and regression analyses were used. The selection of the parameters was based on their role in determining small-scale climate variations (*Adebayo*, 1987; *Oke*, 1987; *Golany*, 1996).

The selected urban parameters were percentage of built-up area (covered surface-building, street, pavement, parking lot, etc.) and water surface by grid cells, as well as distance to the city centre (grid cell labeled by C, see Fig. 3).

This distance can be considered as an indicator of the location of a cell within the city. These three parameters are constants for the complete (one-year long) measurement period. However, in each cell their values vary from place to place within the city. They are constants temporally but variables spatially. Searching for statistical relationships, we will take into account that our parameters are at once variables and constants.

The ratio of the built-up area to the total area by grid cells in 25% increments is displayed in *Fig. 4*. Fig. 4 shows, that, for example, the location of the River Tisza (low built-up ratio) is clearly recognised with its east-to-south curve in the south-eastern part of the study area (see also Fig. 2).

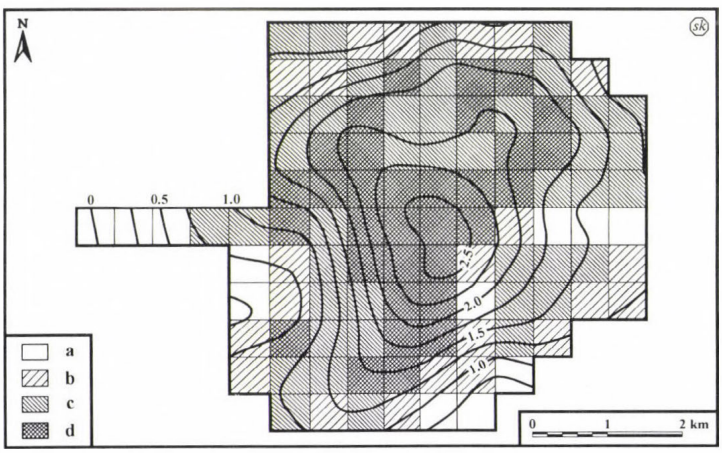

Fig. 4. Spatial distribution of the mean maximum UHI intensity (°C) and the built-up density of the study area by grid cells (ratio of the built-up area to the total cell area) (**a**) 0–25%, (**b**) 25–50%, (**c**) 50–75% and (**d**) 75–100%) during the studied one-year period (March 1999–February 2000) in Szeged.

3. Result and discussion

3.1 Spatial distribution of the maximum UHI

In our investigation not only the one-year period is studied, but within this period we distinguish the so called heating (between October 16 and April 15) and non-heating (between April 16 and October 15) seasons.

It can be seen in *Figs. 4, 5* and *6* that built-up density has a significant influence on the spatial patterns of the mean maximum UHI intensity (4 hours after sunset as supposed). The most obvious common features of these patterns

are that the isotherms show almost regular concentric shapes with values increasing from the outskirts toward the inner urban areas. A vigorous deviation from this concentric shape occurs in the north-eastern part of the city, where the isotherms stretch toward the suburbs. This can be explained by the influence of the large housing estates with tall concrete buildings located mainly in the north-eastern part of the city with a built-up ratio higher than 75% (Fig. 2).

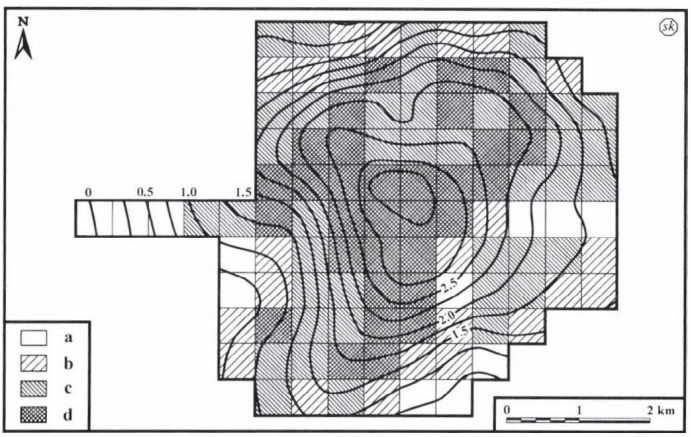

Fig. 5. Spatial distribution of the mean maximum UHI intensity (°C) during the non-heating season (April 16–October 15) in Szeged.

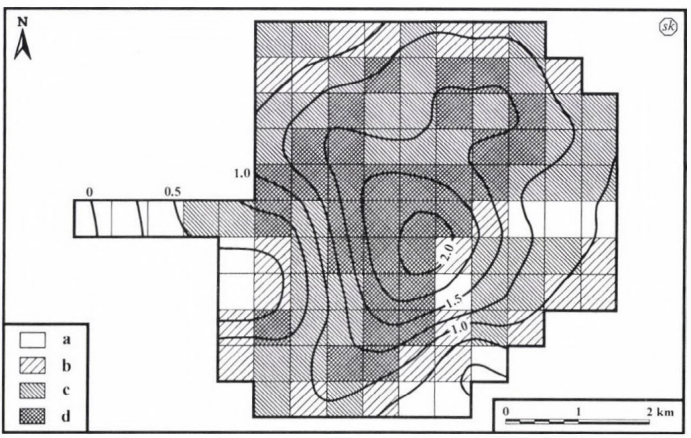

Fig. 6. Spatial distribution of the mean maximum UHI intensity (°C) during the heating season (October 16–April 15) in Szeged.

For the one-year period (Fig. 4), as it was expected, the highest differences (more than 2.5°C) are concentrated mainly in the densely built-up city center (>75%) covered by about 2.5 grid cells (about 0.6 km^2). The strongest intensity (2.60°C) occurs in the central grid cell (C). A mean maximum UHI intensity of higher than 2°C indicates significant thermal modification. In this period in Szeged, the extension of the area, characterized by significant thermal modification, is about 19 grid cells (4.5–5.0 km^2), which is about 18% of the total investigated area.

In the non-heating season, the spreading out of the isolines of 2.25°C and 2.5°C to the north-west of the center, and the isolines of 1.5°C and 1.75°C to the south-west are also caused by the high built-up ratio of more than 75% (Fig. 5). The highest differences (more than 2.75°C) are concentrated in the densely built-up city center (>75%) covered by about 8 grid cells (2 km^2). The greatest intensity (3.18°C) is to the north of the central grid cell (C) in an adjacent cell. The mean maximum UHI intensity of higher than 2°C is relatively large compared to the size of the study area. It covers about 40 grid cells (10 km^2), which is about 37% of the investigated area.

In the heating season, the high built-up ratio of more than 75% also caused the streching out of the isoline of 1.5°C to the north-west, and the isolines of 1°C and 1.25°C to the south-west (Fig. 6). The highest differences (more than 2°C) are concentrated in the city centre (>75%), covered by less than 2 grid cells (0.5 km^2), which is only about 2% of the total area. The strongest intensity (2.12°C) occurs in the central grid cell (C).

The seasonal differences may be formed as a consequence of different weather characteristics in the two seasons rather than as a consequence of heating or non-heating of inhabitants. This explanation is supported by *Klysik* and *Fortuniak* (1999), who found similar differences in the UHI intensities between warm and cold seasons in Łódź, Poland. As in Poland, in Hungary (particularly in the Szeged region) the climate conditions in winter, conducive to the formation of UHI, are less common (Table 1). Thus, in the warmer, therefore non-heating season, the role of appropriate weather conditions (stronger solar radiation income, more frequent clear sky and weak wind) and the reduced latent heat transport because of the more impermeable and guttered urban terrain is more pronounced in the development of UHI than the building heating in urban areas. Consequently, in case of Szeged, the significance of artificial heating in the development of UHI is rather limited.

3.2 Statistical relationships

In order to determine model equations for the maximum value of UHI intensity in the diurnal temperature course (ΔT), we use the earlier mentioned parameters (their labels are in brackets): distance from the central grid cell in km

(D), ratio of built-up surface as a percentage (B) and ratio of water surface as a percentage (W). These parameters are variables spatially, namely by grid cells, but constants temporally.

The bivariate analysis will be accurate if the total period averages of ΔT for each cell are correlated against each of the cell value of D, B and W, thus the time averages of the maximum UHI intensities vary by grid cells (the number of data pairs is $n = 107$).

Table 3 contains the results of the bivariate correlation analyses on ΔT against the urban surface parameters considered in this study. As the table shows, among the examined parameters D has the largest correlation coefficients ($r_{\Delta T,D}$). This fact supports the establisment in Chapter 3.1 on the regular concentric shapes of the UHI isotherms in Szeged. The first two coefficients (D, B) are significant at 0.1% in all the three periods. The strong relationships between ΔT and D as well as B by periods can be seen in the *Figs. 7, 8* and *9*. The ratio of water surface seems not to be important ($r_{\Delta T,W} < 0.06$ always, so it is not significant even at 10% level), for this reason it is not necessary to be used in the multiple regression equations. This statistically insignificant role of water surfaces (mainly connected with the River Tisza) in the development of the maximum heat island in Szeged can be explained by the relatively large size of the grid cells, therefore, water surfaces can be found only in 39 grid cells from the total number of 107 and their ratio is only few percentages in most of the grids.

Table 3. Values of bivariate correlation coefficients between the average of maximum UHI intensity (ΔT) in °C and urban surface parameters (D – distance from the city center in km, B – ratio of built-up area as a percentage and W – ratio of water surface as a percentage) by grid cells in different periods in Szeged ($n = 107$)

Bivariate correlation coefficient (n = 107)	**March 1999–February 2000**		**April 16–October15 (non-heating season)**		**October 16–April 15 (heating season)**	
	Value	**Significance level**	**Value**	**Significance level**	**Value**	**Significance level**
$r_{\Delta T,D}$	–0.837	0.1%	–0.861	0.1%	–0.760	0.1%
$r_{\Delta T,B}$	0.685	0.1%	0.675	0.1%	0.674	0.1%
$r_{\Delta T,W}$	0.044	–	0.056	–	0.020	–

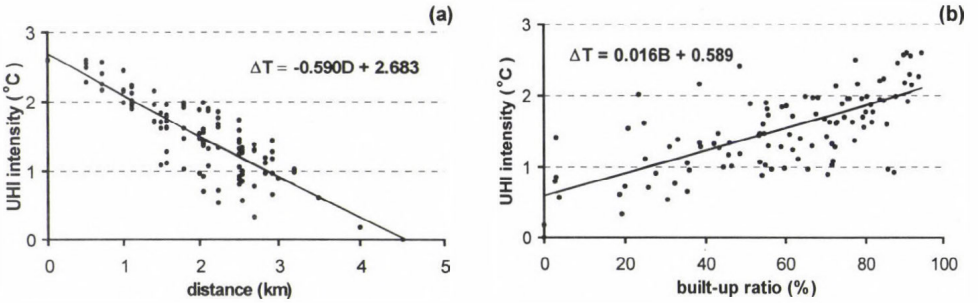

Fig. 7. Maximum UHI intensity (ΔT) as a function of (*a*) the distance from the center (D) and (*b*) built-up ratio (B) with the best fit regression lines in the one-year period (March 1999–February 2000) in Szeged.

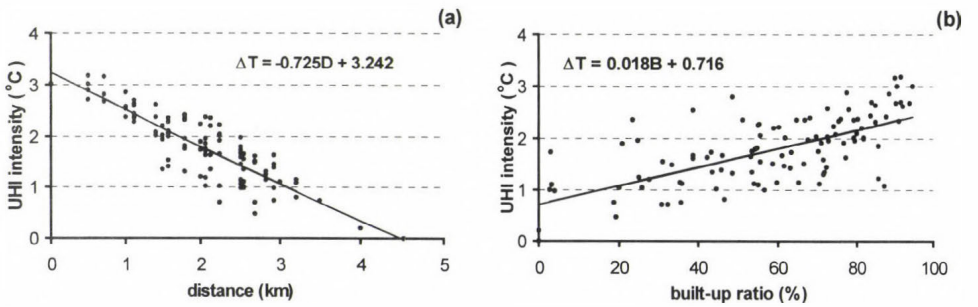

Fig. 8. As *Fig. 7* but in the non-heating season (April 16–October 15).

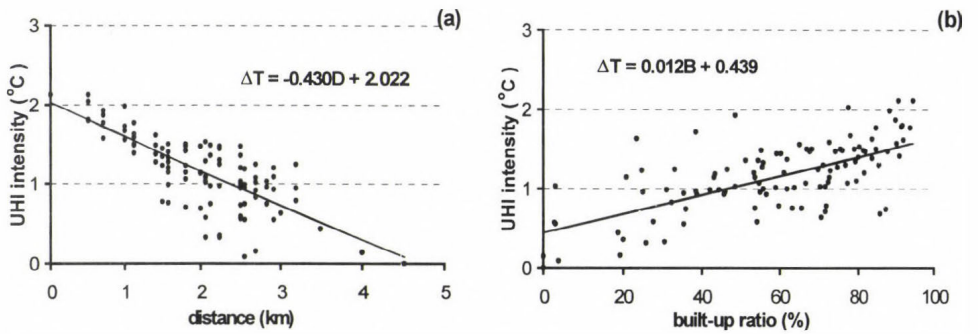

Fig. 9. As *Fig. 7* but in the heating season (October 16–April 15).

The sequence of the parameters, entered in the multiple stepwise regression, was determined with the help of the magnitude of the bivariate correlation coefficients. *Table 4* contains the results of this stepwise regression on ΔT against the urban surface parameters in the three investigated periods. As the results show, the distance from the city center is most pronounced, but the role of the built-up density is also important. The improvements in the explanation caused by entering of B, namely the differences as a percentage in the correlation coefficients in the fourth column of the table (Δr^2) of 6.8%, 5.3% and 15.0% cannot be neglected. The moderate large values of Δr^2 can be explained by the fact that D and B in a city structure are not entirely independent from each other.

Table 4. Values of the stepwise correlation of maximum UHI intensity (ΔT) and urban surface parameters by grid cells in different periods in Szeged (n = 107)

Period	Parameter entered	Multiple $\lvert r \rvert$	Multiple r^2	Δr^2
March 1999–	D	0.837	0.701	0.000
February 2000	B	0.877	0.769	0.068
April 16–October 15	D	0.861	0.742	0.000
(non-heating season)	B	0.892	0.795	0.053
October 16–April 15	D	0.760	0.577	0.000
(heating season)	B	0.816	0.666	0.150

Table 5. Best fit model equations for the average of maximum UHI intensity (ΔT) using urban surface parameters in different periods in Szeged (n = 107)

Period	Parameters	Multiple linear regression equations	Significance level
March 1999–	D	$\Delta T = -0.590D + 2.683$	0.1%
February 2000	D, B	$\Delta T = -0.466D + 0.007B + 2.016$	0.1%
April 16–	D	$\Delta T = -0.725D + 3.242$	0.1%
October 15	D, B	$\Delta T = -0.593D + 0.008B + 2.533$	0.1%
October 16–	D	$\Delta T = -0.430D + 2.022$	0.1%
April 15	D, B	$\Delta T = -0.315D + 0.007B + 1.406$	0.1%

Referring to the investigated periods, *Table 5* contains the model equations which describe ΔT in the best way. The absolute values of the multiple correlation coefficients (r) between the maximum UHI intensity and the parameters are 0.837 and 0.877 for the one-year period, 0.861 and 0.892 for the non-heating season and 0.760 and 0.861 for the heating season (they are all

significant at 0.1% level) (*Tables 4* and *5*). The corresponding squares of these multiple correlation coefficients (r^2) provide explanations of 70.1% and 76.9%, of 74.2% and 79.5 and of 57.7% and 66.6% of the variance, respectively.

4. Conclusions

The seasonal spatial distribution of the maximum urban heat island and its quantitative relationships with urban surface parameters are investigated in the present study. The results indicate that:

- The spatial patterns of the maximum UHI intensity have regular concentric shapes and the isotherms increase from the outskirts towards the central urban areas in all the three studied periods.

- The anomalies in the regularity are caused by the alterations in the built-up density.

- There are significant differences in the magnitudes of the seasonal (heating and non-heating) patterns. The area of the mean maximum UHI intensity of higher than 2°C — indicates significant thermal modification caused by urbanisation — is 18 times larger in the non-heating than in the heating season (2% and 37%, respectively).

- As the correlation coefficients of the parameters show, a short distance from the city center and a high built-up ratio, which prevail mostly in the inner parts of the city, play important roles in the increment of the urban temperature.

Consequently, our preliminary results prove that the statistical approach which determines the behaviour of the UHI intensity in Szeged is promising and this fact urges us to make more detailed investigations. We are planning to extend this project by modeling urban thermal patterns as they are affected by weather conditions with a time lag. We intend to employ the same parameters used in this study, as well as additional urban and meteorological parameters, to predict the magnitude and spatial distribution of the maximum UHI intensity on the days characterised by any kind of weather conditions (apart from the ones with precipitation) at any time of the year without recourse to extra mobile measurements. These tasks require longer-term data sets, so we intend to gather data for a period of more than one year.

The results will be of practical use in predicting the pattern of energy consumption inside the city. They can be used to forecast and plan the energy demand, particularly in cold and warm periods of the year, when energy consumption of heating and cooling, respectively, is highest.

Acknowledgements—The research was supported by the grants of the Hungarian Scientific Research Fund (OTKA T/023042) and the Ministry of Education (FKFP-0001/2000.). The authors wish to give special thanks to the students who took part in the measurement campaigns and in data pre-processing.

References

Adebayo, Y.R., 1987: Land-use approach to the spatial analysis of the urban 'heat island' in Ibadan. *Weather 42*, 272-280.

Boruzs, T. and *Nagy, T.*, 1999: *Urban Influence on the Climatological Parameters* (in Hungarian). MSc thesis, University of Szeged, Szeged, 81 pp.

Chow, S.D., Zheng, J. and *Wu, L.*, 1994: Solar radiation and surface temperature in Shangai City and their relation to urban heat island intensity. *Atmos. Environ. 28*, 2119-2127.

Golany, G.S., 1996: Urban design morphology and thermal performance. *Atmos. Environ. 30*, 455-465.

Goldreich, Y., 1992: Urban climate studies in Johannesburg, a sub-tropical city located on a ridge - A review. *Atmos. Environ. 26B*, 407-420.

Grimmond, C.S.B., Cleugh, H.A. and *Oke, T.R.*, 1991: An objective urban heat storage model and its comparison with other schemes. *Atmos. Environ. 25B*, 311-326.

Grimmond, C.S.B. and *Oke, T.R.*, 1991: An evapotranspiration-interception model for urban areas. *Water Resources Res. 27*, 1739-1755.

Jendritzky, G. and *Nübler, W.*, 1981: A model analysing the urban thermal environment in physiologically significant terms. *Arch. Met. Geoph. Biol. Ser.B. 29*, 313-326.

Johnson, D.B., 1985: Urban modification of diurnal temperature cycles in Birmingham. *J. Climatology 5*, 221-225.

Johnson, G.T., Oke, T.R., Lyons, T.J., Steyn, D.G., Watson, I.D. and *Voogt, J.A.*, 1991: Simulation of surface urban heat islands under 'ideal' conditions at night, I: Theory and tests against field data. *Boundary Layer Met. 56*, 275-294.

Klysik, K. and *Fortuniak, K.*, 1999: Temporal and spatial characteristics of the urban heat island of Łódź, Poland. *Atmos. Environ. 33*, 3885-3895.

Kuttler, W., 1998: *Stadtklima.* In *Stadtökologie* (eds.: *Sukopp, H.* und *Wittig, R.*). *Gustav Fischer, Stuttgart-Jena-Lübeck-Ulm*, 125-167.

Kuttler, W., Barlag, A-B. and *Roßmann, F.*, 1996: Study of the thermal structure of a town in a narrow valley. *Atmos. Environ. 30*, 365-378.

Lillesand, T.M. and *Kiefer, R.W.*, 1987: *Remote Sensing and Image Interpretation.* J. Wiley & Sons, New York, 705 pp.

Mucsi, L., 1996: Urban land use investigation with GIS and RS methods. *Acta Geographica Univ. Szeged 25*, 111-119.

Myrup, L.O., McGinn, C.E. and *Flocchini, R.G.*, 1993: An analysis of microclimatic variation in a suburban environment. *Atmos. Environ. 27B*, 129-156.

Nkemdirim, L.C., 1978: Variability of temperature fields in Calgary, Alberta. *Atm. Environment 12*, 809-822.

Oke, T.R., 1973: City size and the urban heat island. *Atmos. Environ. 7*, 769-779.

Oke, T.R., 1976: The distinction between canopy and boundary layer urban heat islands. *Atmosphere 14*, 268-277.

Oke, T.R., 1987: *Boundary Layer Climates.* Routledge, London and New York, 405 pp.

Oke, T.R., 1997: *Urban climates and global environmental change.* In *Applied Climatology* (eds.: *R.D Thompson.* and *A Perry*). Routledge, London-New York, 273-287.

Oke, T.R. and *Maxwell, G.B.*, 1975: Urban heat island dinamics in Montreal and Vancouver. *Atmos. Environ. 9*, 191-200.

Park, H-S., 1986: Features of the heat island in Seoul and its surrounding cities. *Atmos. Environ. 20*, 1859-1866.

Ripley, E.A., Archibold, O.W. and *Bretell, D.L.*, 1996: Temporal and spatial temperature patterns in Saskatoon. *Weather 51,* 398-405.

Sailor, D.J., 1998: Simulations of annual degree day impacts of urban vegetative augmentation. *Atmos. Environ. 32,* 43-52.

Sundborg, A., 1950: Local climatological studies of the temperature conditions in an urban area. *Tellus 2,* 222-232.

Tapper, P.D., Tyson, P.D., Owens, I.F. and *Hastie, W.J.*, 1981: Modeling the winter urban heat island over Christchurch. *J. Appl. Meteorology 20,* 365-367.

Tumanov, S., Stan-Sion, A., Lupu, A., Soci, C. and *Oprea, C.*, 1999: Influences of the city of Bucharest on weather and climate parameters. *Atmos. Environ. 33,* 4173-4183.

Unger, J., 1996: Heat island intensity with different meteorological conditions in a medium-sized town: Szeged, Hungary. *Theor. Applied Climatology 54,* 147-151.

Unger, J., 1999: Urban-rural air humidity diferences in Szeged, Hungary. *Int. J. Climatology 19,* 1509-1515.

Unger, J., Sümeghy, Z., Gulyás, Á., Bottyán, Zs. and *Mucsi, L.*, 1999: Modeling the maximum urban heat island. *Proceed. ICB-ICUC'99,* Sydney, Australia, ICUC10.4.

Voogt, J.A. and *Oke, T.R., 1991*: Validation of an urban canyon radiation model for nocturnal long-wave radiative fluxes. *Boundary Layer Met. 54,* 347-361.

Voogt, J.A. and *Oke, T.R.*, 1997: Complete urban surface temperatures. *J. Appl. Meteorology 36,* 1117-1132.

Yamashita, S., 1996: Detailed structure of heat island phenomena from moving observations from electric tram-cars in metropolitan Tokyo. *Atmos. Environ. 30,* 429-435.

IDŐJÁRÁS

Quarterly Journal of the Hungarian Meteorological Service
Vol. 104, No. 4, October–December 2000, pp. 269–277

The use of biometeorological forecasting to raise sports achievements

Imre Örményi

International Committee for Research and Study of Environmental Factors, Hungarian Section, Király utca 52, H-1061 Budapest, Hungary

(Manuscript submitted for publication 16 March 2000; in final form 26 June 2000)

Abstract—The author furnished sport biometeorological forecasts to a selected team before each of its matches during the indoor handball championship in the men's premier league of Hungary in 1990/1991. The players' individual weather sensitivity was established prior to the championship. Keeping this in mind, the outcome of earlier studies on the interrelationship between sports achievements and various weather phenomena and alterations in solar activity and/or geomagnetism made possible to predict alterations of the players' nervous state and their expected individual performances. Particular attention was paid to the goalkeepers' performances and the expected changes of their reaction time. As a result of the applied procedure the selected handball team won the championship, moving from the fifth place to the first.

Key-words: handball players, sporting activity, biometeorological forecasting.

1. Introduction

Sport specialists are more or less familiar with the investigations of influence of certain climates on sports and their practical use. It is less known, however, that alterations of weather components, especially those with frontal passages have influence on sport performance too. Such investigations were carried out in Hungary on marksmen (*Horváth,* 1960), male handball players (*Örményi* and *Ried,* 1966), on Hungarian sprinters and long-distance runners, discus and hammer throwers and high jumpers (*Miltényi* and *Kereszty,* 1966). Most recently *Örményi* (1991) investigated the physiological reactions and performances of representative ice hockey goalkeepers.

To compensate the players' possible bad performances, benefit of forecasting of sport achievements can be a useful tool. Compensation is possible by substituting some of the players for others and resort new tactics.

Sport meteorological forecast was first tested on an ice hockey goalkeeper of the national team on December 9, 1961 in the Kisstadion of Budapest. The forecast was tested after founding interrelations between weather elements and sport achievements. On that particular occasion, after completing on him the appropriate medical examinations, the goalkeeper's excellent performance was expected, and in fact he reached an extremely good result of 91% as compared to his 63% performance averaged over the entire ice hockey season. (Performance means the scores divided by the number of shots reaching the goal.)

Since that time our intuition concerning reality of raising sports achievements by the use of biometeorological forecasts has been confirmed by the relevant research on the matter. This time we investigated the use of biometeorological forecasts during a complete indoor handball championship. This type of sport had been investigated before, so we could apply the results to test the forecasts serially.

2. Methods and used material

Complex effect of meteorological, biological and psychological factors on the performance of indoor handball players was investigated in details by *Örményi* and *Ried* (1966). During the winter championship of the national handball league in 1958/1959, were the three top teams of Hungary, named Honvéd of Budapest, Elektromos of Budapest and Kábelgyár of Budapest, investigated.

The authors considered endogenous and exogenous factors that have influences on sports achievements. Physical state of the contestants, stage fright, circadian rhythm of the organism and the sportsmen's health state were counted among endogenous factors. Exogenous factors were those characterized by changes in the outside world, e.g., referees, spectators, climatic and meteorological factors. Investigations were extended to the physiological functions, psychological state, meteorological conditions, players' sporting achievements.

The following meteorological factors were taken into consideration: dry and wet bulb temperature, relative humidity, vapor pressure of the air, air movements, cooling power[1], the equivalent temperature, the effective temperature, air pressure tendency, various types of frontal passages, air masses near the surface and vertical motions.

Records were made about the successful actions and those with no success, directions and strengths of shots, shortened playing time because of substitution or referees' bad judgements, number of offensive and defensive actions were summed up.

[1] Measured by katathermometer providing a value on the complex effect of air temperature, humidity and air flow.

All the data recorded were systematized and analyzed according to Schelling's T-method (*Schelling,* 1940). For better understanding *Table 1* presents the T-values characterising the interrelationships between frontal passages and the playing elements in handball (*Örményi* and *Ried*, 1966). We took into consideration happenings ± 10 hours around the front passage.

Table 1. Interrelationships between frontal passages and the playing elements in handball

Playing elements	Frontal passages					
	Warm front		Cold front		Subsidence	
	before	after	before	after	before	after
Performance*	-2.2	0.7	2.37	0.19	–	-0.47
Efficiency from the first half to the second one*	-2.31	-0.43	1.67	0.38	–	-1.16
Mishit*	-1.14	-1.84	-0.20	0.03	–	2.15
Goal*	-1.84	2.10	-0.99	-0.96	–	-0.94
Total number of shots	20.6	18.6	18.5	24.3	–	17.9
Number of attacks	18.8	23.1	21.3	21.3	–	21.5

* If $T=1.96$ the probable error is $P=0.05$. In case of $T=3.0$ the probable error level is $P=0.0027$

Table 1 indicates that performances as well as the players' efficiency in the second half of the game significantly decrease *before a warm front passage* and the number of goals is remarkably less due to the increased errors in aiming.

After a warm front passage performance and efficiency for the second half of the game increase in relation to the prefrontal situation. Number of attacks and the number of goals are the highest (probable error level $P<0.05$).

The players' performance and the efficiency are the best ($P<0.05$) *before a cold front passage*, though they are not very active (number of shots and attacks are relatively low), and the goals are below the average level.

After a cold front passage performance and efficiency changes are around the average. Shots are very numerous but the rate of success is not good at all.

Nothing can be said about the figures before a divergence (subsidence), as no such cases were observed during the investigated period.

Performance decreases *after a divergence*. A remarked lack of concentration resulting in high number of mishits ($P<0.05$) can be experienced and the number of shots is the smallest at the same time.

Considering the *air masses on the ground level,* performance significantly increases ($P<0.05$) during *subtropical air masses*. In *maritime Arctic air masses* the performance is negative ($T=-1.38$) compared to the average level.

If there is a warm advection in the higher levels of the troposphere with a sudden subtropical influx, the achievements seem to be the worst ($T=-3.40$). Compare this with the figures before warm front passages. If there is no influx of subtropical air masses or warm front or advection in the higher levels of the troposphere, accomplishments seem to be the best ($T=2.97$).

These results can be applied only to those teams where most of the players are warm front sensitive. These results were applied to the first division of the team Elektromos during a whole handball season from September 29, 1990 to April 28, 1991.

3. Weather sensitivity

It can be determined by various methods such as filling out a questionnaire (*Örményi,* 1972), inhalation of artificial air ions of various polarity (*Örményi, et al.*, 1981) or visual inspection of videoclips based on anthropogenic determination of weather sensitivity types according to *Curry* (1969). Prior to the first match we have determined the type of weather sensitivity by two methods. The first one consisted of filling out a questionnaire based on elaboration of answers of 26,000 Hungarian citizens (*Örményi,* 1972, 1987). The results were published in journal Időjárás (*Örményi*, 1993).

Table 2. Weather sensitivity of Budapest population and numbers of the selected team (in percent)

Sensitivity	Budapest population	Selected team's members
Cold front	29.5	18.8
Mixed front	19.3	18.8
Mixed front	51.2	62.5

The second test was based on inhalation of artificial air ions of various polarity (*Örményi et al.,* 1981). The reason of the ion inhalation was the following. Our former natural atmospheric ion measurements carried out in Budapest at the Danube riverside (opposite to the Margaret Island in Buda), have proved, that the unipolarity coefficient ($q = n+/n-$ where n is the number of ions in 1 ccm) was below 1 during the first day of inflow of Arctic

air masses, which means negative ion preponderance against positive one in the medium small ion range. (The limit mobility $K_g = 1.9 \times 10^{-2}$ cm^{-2} Vsec). During an influx of subtropical air masses, the preponderance of positive ions seems to be in excess to negative ones (*Örményi*, 1967).

During the inhalation of artificially generated ions (by a Medicor made bipolar type ionizator), we have measured blood pressure and pulse rate and calculated the vegetative index[2] (V.I.) of *Kérdő* (1966). If V.I. < 0, vegetative reactions tend to orthostatic (vagotonic), if V.I. > 0, then to sympathetic form of reactions. Generally the trend in physical burden is more expressive. The standard error of vegetative index calculated from measurement of 1000 healthy sportsmen was ± 13 units. This index showed differences (5–50 units of vegetative index) during inhalation of ions of different polarity. The type of weather sensitivity can be determined during inhalation of positive or negative ions as follows: Prior to the inhalation of ions[3] (25 cm away from the mouth) p and d values are measured, then 5 minutes after the inhalation of ions another measurement (p and d) follows. This is followed by a 15-minute recovery period (adaptation and normal breathing without artificial ions). Calculus of pulse and measurement of diastolic pressure follow again, so we obtain 3–3 V.I. values.

The type of weather sensitivity gives that type of ion polarity, where the vegetative tone trends to sympathetic tone. *In case of warm front sensitivity, this situation occurs during positive ion preponderance, meanwhile in case of cold front sensitivity, during negative ion preponderance. In case of mixed type weather sensitivity, the burden of both type of ion polarity results in a similar trend in vegetative index.*

The type of weather sensitivity of top players of rival teams had been determined. This was applied before each derby using video records of the mentioned teams such as BRAMAC (Fotex) Veszprém, RÁBA ETO from Győr and Tatabánya. This procedure was based on anthropogenic determination of the types of weather sensitivity according to *Curry* (1969). Having these results there was a possibility to change tactics.

4. Danger of injury

Ambulance cases including sports accidents and changes of the 3 Hz ELF sferics level in Budapest were investigated by *Örményi and Majer* (1985) on the basis of a vast amount of data. The outcome of this investigation is of

[2] V.I. $= (1 - d/p) \times 100$, where d = the diastolic blood pressure in mmHg, p = the pulse rate during 1 minute.

[3] The ion flux was 50,000 ion/ccm of small ions.

prognostic significance. The mathematical-statistical analysis showed that the number of sports accidents significantly increases if the sferics level decreases by 50% on successive days.

5. Forecasting

Prior to each match the first trainer got a forecast for the following factors: (l) Types of expected weather changes, i.e., frontal passage, subsidence, situation without fronts. (2) Types of expected air masses near the ground — according to *Berkes* (1961). It should be noted, that the unipolarity coefficient differs in various biologically active air masses. (3) During disturbed weather conditions, the expected tendency of visual reaction time of each goal keeper (shortened or prolonged). (4) The character of play: quiet, average, tense atmosphere with rudeness or overhastiness with inaccurate ball technique. (5) Bad or good achievements of certain top players, especially before hard games. (6) Possibility of danger of injury during the match. (7) There was also a forecast during a geomagnetic storm referring to the expected general stress condition. This was measured by indirect method, namely with alteration of natural secondary gamma radiation and ELF sferics on 3 Hz range measured in my former institute (National Institute for Rheumatics and Physiotherapy, Budapest).

6. Philosophy

The basic idea of this experiment was to provide regular biometeorological forecast for the coach of a selected handball team who showed interest in learning its use and saw the changes in the team's achievements.

7. Results and discussion

On the basis of the measurements of weather sensitivity types, it was established, that 10 players belonged to different subtypes of warm front sensitivity, 3 to mixed front sensitive type and 3 to cold front sensitive type. Previous experiences have shown that among top trained contestants, weather sensitivity seems to be rather rare (*Örményi* and *Ried*, 1966). In spite of that, in this study 4 players proved to be strongly labile and other 2 were near to this condition.

It should be noted, that the distribution of weather sensitivity of the questioned 26,000 people was similar to that of the selected team (Table 2).

Since the percentage distribution of warm front sensitive players was

62.5%, there was a positive deviation contrary to the average distribution of our previous elaboration.

The long term biorhythm, according to Fliess was was taken into consideration in the absence of biologically active weather situations. In disturbed weather situations, however, there is no such significance of biorhythm as we could show at ice hockey players (*Örményi*, 1990).

According to the visual reaction time measurements of *Ried* (1971), a good relationship was established during a frontal passage. The reaction time of warm front sensitive people significantly increased at the time of warm front passages ($P<0.01$).

Cold front sensitive people had an increased reaction time during cold front passages ($P<0.05$).

The reaction time of mixed type people (they are sensitive to both types of frontal passage) increased, but not significantly.

This result seems to be of *primer importance* considering the performance of goal keepers. If the reaction time is longer than generally (average level), the goal keeper cannot reach the shot arriving at door.

Sport-biometeorological forecasting was furnished 26 times (*Table 3*). It should be noted, that only the forecast of warm or cold front passages does not furnish any information on expected sporting behaviour and performance. Naturally at the start of the work there was some difficulties in teaching the coaches, who accepted the forecast with scepticism. Later the situation has changed. The trainer got information by phone before matches on strange ground, too.

The championship was won by the team of Elektromos. It should be noted, that a year before the experiment, the mentioned team was on the fifth place at the end of the championship. According to the leaders of the Hungarian Handball Association, the team of Elektromos did not consist of the best players, and in spite of this, *they won the championship*.

In absence of forecast the team of Elektromos finished on the second place in the 1991/1992 and 1992/1993 championships, and finally in the 1993/1994 championship they finished only at *the third place* and remained at the same level. On the other hand there were foreign professional players too, while formerly only Hungarians played in the team.

8. Conclusions

To furnish a sport biometeorological forecast and apply the notices, it is necessary to work with the competitors and *educate the trainers* to the manifestation of influence at the team work. The primary need is to achieve fitness and high level trained conditions of the players.

Table 3. Survey of the matches and the relevant biometeorological forecasts

Date	Match place	Opponent	Scores	Front[a]	Air mass[b]	Reaction time	Game-character	Der-by	In-jury	Geomag-netism
1990										
Sep 29	Dunaújváros	Dunaferr	22-27	W	cA	short	quite	-	-	-
Oct 3	Budapest	Debrecen	20-14	Wu	mC	short	average	-	+	-
Oct 5	Budapest	Szolnok	33-17	C	mW	average	quiet	-	-	-
Oct 12	Várpalota	Várpalota	17-23	-	cT	average	tense	-	+	disturbance
Oct 18	Budapest	Pécs	31-22	C_u	mW	long	tense	-	+	-
Oct 21	Nyíregyháza	Nyíregyháza	24-24	C	cA	long	tense	-	+	-
Nov 2	Budapest	Tatabánya	28-23	C	mM	long	quiet	+	+	disturbance
Nov 11	Szeged	Tisza Volán	23-23	-	cC	long	tense	+	+	storm
Nov 23	Budapest	Bramac	26-23	I	mT	average	tense	+	+	disturbance
Nov 25	Budapest	Rába ETO	25-15	C_u	mT	long	tense	+	+	disturbance
Dec 2	Békéscsaba	Békéscsaba	19-24	Wa	mA	average	quiet	-	-	-
Dec 7	Budapest	Komló	35-27	W	mM	long	quiet	-	-	-
Dec 9	Solymár	Pemű Honv.	17-16	W	mM	short	quiet	-	-	-
1991										
Jan 22	Tatabánya	Tatabánya	27-26	C	cM	long	tense	+	+	-
Jan 27	Budapest	Tisza Volán	33-15	C_u	cC	average	tense	+	-	-
Feb 24	Győr	Rába ETO	20-19	-	cM	average	tense	+	-	-
Feb 28	Veszprém	Bramac	19-19	W_u	cC	short	tense	+	-	disturbance
Mar 3	Budapest	Békéscsaba	37-23	C	mA	long	average	-	-	-
Mar 10	Komló	Komló	20-27	-	mM	average	quiet	-	-	-
Mar 17	Budapest	Pemű Honv.	25-17	-	mT	short	quiet	-	+	disturbance
Mar 22	Debrecen	Debrecen	21-21	W_u	mT	average	tense	-	+	disturbance
Mar 29	Budapest	Dunaferr	33-17	W	mA	short	tense	-	-	-
Apr 6	Szolnok	Szolnok	19-20	I	cT	average	tense	-	+	disturbance
Apr 14	Budapest	Várpalota	22-17	-	mC	short	quiet	-	-	-
Apr 21	Pécs	Pécs	21-21	C	cA	long	tense	-	-	-
Apr 28	Budapest	Nyíregyháza	28-19	-	mC	average	average	-	-	disturbance

a : W=warm front, W_u=upper warm front, C=cold front, C_u=upper cold front, I=instability line

b : mA=maritime Arctic, cA=continental Arctic, mC=maritime cold, cC=continental cold, mM=maritime mild, cM=continental mild, mW=maritime warm, mT=maritime sub-tropical, cT=continental subtropical

References

Berkes, Z., 1961: Luftmassen und fronttypen in Karpathenbecken (in Hungarian). *Időjárás* 65, 289-293.

Curry, M., 1969: *Schlüssel zum Leben*. Schweiz. Verlaghaus. A.G. Zürich.

Horváth, L. G., 1960: *Some Results of Sportphysiological Investigation During Shotter Racing* (in Hungarian). Scientific Books of Sport Council, Budapest.

Kérdő, I., 1966: Ein aus Daten der Blutzirkulation kalkulierter Index zum Beurteilung der vegetativen Tonuslage. *Acta Nettrovegetativa 29*, 250-268.

Miltényi, M. and *Kereszty, A.*, 1966: Interrelations between meteorological frontal passages and 10 years athletic records (in Hungarian). *Testnevelési Főiskola Közlemények*, 85-96.

Örményi, I., 1967: Investigations of atmospheric ionisation in surroundings of St. Lucas Spa. *Annales of the Hungarian Balneoclimatological Society*, Budapest, 105-129.

Örményi, I., 1972: Questionnairy method for determination of sensitivity for weather (in Hungarian). *Ergonomia* 5 (2), 156-165.

Örményi, I., 1987: Variation of weather sensitivity (Geophysical Biotopology) over 40 years among representative population of Budapest (in Hungarian). *Publ. of the National Institute of Rheumatology and Physiotherapy*. Budapest, 169 p.

Örményi, I., 1990: Alteration in performance and some physiological parameters on ice hockey players due to their biorhythms according to Fliess. *Proc. Symp. of Human Biometeorology*. Strbské Pleso, 1989, 297-304.

Örményi, I., 1991: Biometeorological investigation of representative ice hockey goal keepers (in Hungarian). *Physical Education and Sport Science*. Budapest, 22. 22-27, 35-41.

Örményi, I., 1993: An advanced accidents forecasting technique based on weather sensitivity of drivers. *Időjárás* 97, 187-200.

Örményi, I. and *Majer, J.*, 1985: Ambulance cases and changes of the 3 Hz static levels (ELF sferics) in Budapest (in Hungarian). *Magyar Mentésügy 5*, 165-173.

Örményi, I., Megyer, M. and *Nyíri, L.*, 1981: One possibility of determination of adaptation of man depending on individual geophysical-biotopology useing artificial atmospheric ions. *Abstract. Vol. 9th International Congress of Biometeorology*. 1980. Osnabrück. Swets and Zeitlinger. 70. p.

Örményi, I. and *Ried, J.*, 1966: Complex effect of meteorological, biological and psychological factors on the performance of indoor handball players (in Hungarian). Copies of the Scientific Council of Physical Education. Budapest. 120 p.

Ried, J., 1971: Influence of weather on psychical factors and sporting achievements (in Hungarian). Thesis for Ph.D. Hungarian Academy of Sciences, Budapest.

Schelling,. H., 1940: Arbeiten aus dem Staatlichen Institut für experimentelle *Therapie und dem Forschungsinstitut für Chemotherapie*. No. 39. 35.S.

IDŐJÁRÁS

VOLUME 104 * 2000

BUDAPEST, HUNGARY

AUTHOR INDEX

TABLE OF CONTENTS

I. Papers

II. Book review

III. Contents of journal Atmospheric Environment, 2000

IV. SUBJECT INDEX

The asterisk denotes book reviews

G

H

L

M

N

O

P

Q

R

S

T

U

W

Y

NOTES TO CONTRIBUTORS OF *IDŐJÁRÁS*

The purpose of the journal is to publish papers in any field of meteorology and atmosphere related scientific areas. These may be

- reports on new results of scientific investigations,
- critical review articles summarizing current state of art of a certain topic,
- shorter contributions dealing with a particular question.

Each issue contains "News" and "Book review" sections.

Authors may be of any nationality, but the official language of the journal is English. Papers will be reviewed by unidentified referees.

Manuscripts should be sent to
Editor-in-Chief of IDŐJÁRÁS
P.O. Box 39
H-1675 Budapest, Hungary

in three copies including all illustrations. One set of illustrations has to be of camera ready quality, the other two might be lower quality.

Title part of the paper should contain the concise title, the name(s) of the author(s), the affiliation(s) including postal and E-mail address(es). In case of multiple authors, the cover letter should indicate the corresponding author.

Abstract should follow the title, it contains the purpose, the data and methods as well as the basic conclusion.

Key-words are necessary to help to classify the topic.

The text has to be typed in double spacing with wide margins. Word-processor printing is preferred. The use of SI units are expected. The negative exponent is preferred to solidus. Figures and tables should be consecutively numbered and referred to in the text.

Mathematical formulas are expected to be as simple as possible and numbered in parentheses at the right margin. Non-Latin letters and hand-written symbols should be indicated and explained by making marginal notes in pencil.

Tables should be marked by Arabic numbers and printed in separate sheets together with their captions. Avoid too lengthy or complicated tables.

Figures should be drawn or printed in black and white, without legends, on separate sheets. The legends of figures should be printed as separate list. Good quality laser printings are preferred as master copies.

References: The text citation should contain the name(s) of the author(s) in Italic letter and the year of publication. In case of one author: *Miller* (1989), or if the name of the author cannot be fitted into the text: *(Miller,* 1989); in the case of two authors: *Gamov* and *Cleveland* (1973); if there are more than two authors: *Smith et al.* (1990). When referring to several papers published in the same year by the same author, the year of publication should be followed by letters a,b etc. At the end of the paper the list of references should be arranged alphabetically. For an article: the name(s) of author(s) in Italics, year, title of article, name of journal, volume number (the latter two in Italics) and pages. E.g. *Nathan, K.K.,* 1986: A note on the relationship between photosynthetically active radiation and cloud amount. *Időjárás 90*, 10-13. For a book: the name(s) of author(s), year, title of the book (all in Italics except the year), publisher and place of publication. E.g. *Junge, C. E.,* 1963: *Air Chemistry and Radioactivity*. Academic Press, New York and London.

The final version should be submitted on diskette altogether with one hard copy. Use standard 3.5" or 5.25" DOS formatted diskettes. The preferred word-processors are WordPerfect 5.1 and MS Word 6.0.

Reprints: authors receive 30 reprints free of charge. Additional reprints may be ordered at the authors' expense when sending back the proofs to the Editorial Office.

More information: gmajor@met.hu
Information on the last issues:
http://www.met.hu/firat/ido-e.html

Published by the Hungarian Meteorological Service

Budapest, Hungary

INDEX: 26 361

HU ISSN 0324-6329